Constitutive RIG-I activation causes skin lesion resembling psoriasis in transgenic mice

AHMED S.A. ABU TAYEH

Table of contents

Abstract

Psoriasis is a chronic immune-mediated skin disease affecting 2-3% of population worldwide. Retinoic acid Inducible Gene I (RIG-I), a cellular protein that recognizes viral RNA in the immune and non-immune cells, has recently been linked with the development of some autoimmune diseases, including psoriasis. Here I report spontaneous development of psoriasis-like disease in a transgenic mice harboring mutated human copy of the gene *DDX58* (encoding RIG-I) with one single-base substitution A1118C causing amino acid exchange in human RIG-I (hR) E373A (c.1118A>C [p. Glu373Ala]), causing a gain-of-function mutation. Histological analysis showed typical characteristics of psoriasis including increased epidermal proliferation, abnormal differentiation and infiltrates consisting T cells, neutrophils and dendritic cells. The lesion was innate-immune dependent, and intercrossing the transgenic mice with type I IFN receptor-deficient mice (hR E373A *Ifnar1*$^{-/-}$) or mitochondrial antiviral signaling protein-deficient mice (hR E373A *Mavs*$^{-/-}$) mice has completely abolished the phenotype, suggesting direct RIG-I involvement. The lesion showed elevated levels of the IL-23/IL-17 immune axis cytokines, and while IL-17A deficiency abolished the phenotype, hR E373A *Rag2*$^{-/-}$ transgenic mice did not abolish the lesion but ameliorated it indicating a role for nonlymphoid cells in the development of the phenotype. Results provide another evidence for the implication of RIG-I in psoriasis-like skin disorder and systemic auto inflammatory disease.

Abbreviations

AGS	Aicardi-Goutieres syndrome
CM	Commensal microbiota
DDX58	DExD/H-box helicase 58
GOF	gain-of–function
IFIH1	interferon induced with helicase C domain 1
IFNAR1	interferon alpha and beta receptor subunit 1
ILC3s	group 3 innate lymphoid cells
IMQ	Imiquimod
IRF3	interferon regulatory factor 3
IRF7	interferon regulatory factor 7
K5	keratin 5
K6	keratin 6
K16	keratin 16
LGP2	laboratory of genetics and physiology 2
MAVS	mitochondrial antiviral signaling protein
MCP-1	monocyte chemoattractant protein-1
MDA5	melanoma differentiation-association protein 5
MS	multiple sclerosis
NF-κB	nuclear factor-κB
Rag2	recombination activating gene 2
RIG-I	retinoic acid-inducible gene I
RLR	RIG-I like receptor
RORγt	retinoic acid receptor-related orphan receptor γt

SLE	systemic lupus erythematosus
SMS	Singleton-Merten syndrome
SNP	single-nucleotide polymorphism
STAT3	signal transducer and activator of transcription 3
Tg	transgenic
Tgfb	transforming growth factor beta
Tnfa	tumor necrosis factor alpha
VEGF	vascular endothelial growth factor

Chapter 1

INTRODUCTION

1.1 RIG-I like receptors role in innate immunity

Innate immunity is the first line of defense against invading viruses. Cells of the innate immune system detect viral infection through the pattern recognition receptors (PRRs) that sense microbe-associated molecular patterns (MAMPs) (1), molecules that are conserved in whole classes of microbes but are absent from the host exhibited by pathogens. PRRs are either on the cell surface or within distinct intracellular compartments (1) and upon recognizing a viral nucleic acids, they trigger the production of interferon (IFN) and many other proinflammatory cytokines (1).

RIG-I like receptors (RLR) are a group of cytosolic proteins that work as pathogen recognition receptors (PRRs) inside immune and non-immune cells (2). RLR family includes Retinoic Acid Inducible Gene I (RIG-I), Melanoma Differentiation Associated gene 5 (MDA5), Laboratory of Genetics and Physiology 2 (LGP2). They are essential in recognizing viral RNAs, and initiating signaling cascades that involve promotion of transcriptional factors interferon regulatory factor 3 (IRF-3), IRF-7 and nuclear factor κB (NF-κB) factors, resulting in the expression of type I interferons and other proinflammatory cytokines (Fig. I). This induces an anti-viral state in the infected and surrounding cells, and the initiation of the acquired immune response to fight invading pathogens (2).

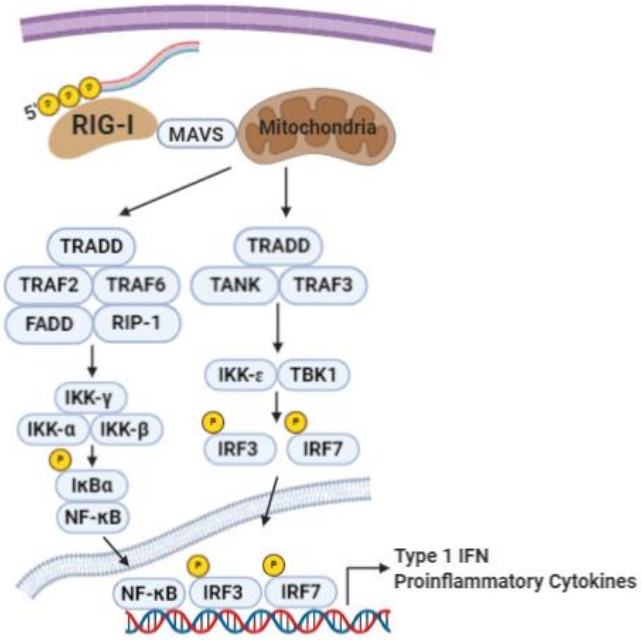

Figure I: RIG-I viral detection and induction of antiviral signaling pathway

The cytoplasmic pattern-recognition receptor RIG-I recognizes RNA viruses with a 5'ppp signature. Upon recognition, RIG-I recruits the adaptor protein mitochondrial antiviral signaling protein to activate the TBK1–IKKϵ complex and IKKα–IKKβ complex, which are responsible for the activation of transcription factors interferon regulator factor 3 (IRF3), IRF7 and nuclear factor-κB. These transcription factors then translocate to the nucleus and coordinate the expression of type I interferons (IFNs) and other pro-inflammatory cytokines.

1.2 RIG-I like receptors involvement in autoimmune diseases

Many studies have implicated the RLRs in the pathogenesis of many autoimmune diseases, such as diabetes mellitus (3) , multiple sclerosis (4), psoriasis (5), dermatomyositis (6), selective IgA deficiency (7) and Systemic lupus erythematosus (SLE) (8-10). Our laboratory previously revealed in a mouse model that a missense mutation in *Ifih1* gene (Interferon-induced helicase C domain1) which encodes MDA5 G821S was enough to cause lupus-like symptoms (11) and bone abnormalities though constitutive production of type I IFNs (12). Other 3 missense mutations in *IFIH1* have been identified to cause Aicardi-Goutieres syndrome, a rare progressive

autoinflammatory disorder that predominantly causes encephalopathy (13). The mutations caused an excessive production of type I interferon and the transcription of interferon-stimulated genes (ISGs) (13). Luciana *et al.* also identified two families with musculoskeletal manifestations marked by up-regulation of type I IFN as a result of a gain-of-function (GOF) mutation in *IFIH1* gene (14). Blockade of Janus kinases 1 and 2 by ruxolitinib in patients with progressive neurological and lupus-like disease due to the *IFIH1* mutation showed symptomatic and clinical improvement (15). Moreover, SNPs in the gene *DDX58*, which encodes RIG-I, were linked with MS and SLE, and psoriasis susceptibility has also been reported (4, 16, 17).

1.3 RIG-I like receptors involvement in Singleton-Merten syndrome (SMS)

SMS is a rare autosomal dominant multisystemic autoinflammatory disorder that develops in early childhood at the age of approximately 4 months- to 2 years old (18). The classic type of the disease is characterized by cardiovascular manifestations (calcifications in the heart valves and aorta), skeletal abnormalities (osteoporosis, osteopenia, joint subluxation and acroosteoysis) and dental abnormalities (short dental roots, tooth and alveolar bone resorption, truncated root formation, high rate of caries and tooth loss). Less common features may include glaucoma, psoriasis, muscle weakness and atrophy, developmental delay and short stature (19). Rutsch et al. reported a common missense GOF mutation (R822Q) in the helicase 2 domain of the *IFIH1* gene in two different families and a simplex case (20) of previously reported SMS patients. Likewise, other reports have also supported the involvement of MDA5 in the pathogenesis of SMS (18, 21, 22).

In addition to the association of MDA5 to SMS, RIG-I have also been implicated. A study described two mutations in DEAD box polypeptide 58 (*DDX58*) gene which encodes RIG-I E373A and C268F in SMS patients of two different families. Patients with RIG-I E373A mutation are

complicated with aortic calcification, glaucoma and skeletal abnormalities, but in contrast to classic SMS patients, they had no dental manifestations, suggesting an atypical form of SMS. Structural analysis revealed that the Glu373 residue belongs to the ATP-binding motif II close to the ADP and RNA molecules (23). Based on the *in vitro* experiments, the missense mutation E373A activated the RIG-I signaling pathway, leading to the induction of transcription factor *NF-κB*, *IFNB1* and *ISG15* genes even in the absence of a stimulus, suggesting a GOF state (23). This GOF state was due to prolonged self-RNA binding (24), however, the exact molecular mechanism by which RIG-I SMS mutants induce signaling here have not been clarified.

To examine how hR E373A mutation causes human autoinflammatory disease, our laboratory generated transgenic mice harboring mutated human copy of *DDX58* with one single-base substitution A1118C causing amino acid exchange in human RIG-I E373A. Data shows that around one third of mice with hR E373A Tg developed skin lesion resembling human psoriasis through the activation of the IL-23/IL-17 immune axis. Though IFN-β expression was not noticed, the lesion was innate-immune mediated and hR E373A *Ifnar1*$^{-/-}$ Tg mice showed no abnormality in the skin. Along with the high expression of cytokines of RIG-I signaling pathway and IL-23/IL-17 immune axis, dendritic cells and T cells infiltrates were noticed, while hR E373A *Il17*$^{-/-}$ Tg mice showed normal skin. Amelioration, but not absence, of the skin phenotype in hR E373A *Rag2*$^{-/-}$ mice was noticed, indicating the involvement of nonlymphoid cells in the pathogenesis of the disease. This lesion was associated with systemic inflammation and comorbidities in other organs.

Chapter 2

MATERIALS AND METHODS

2.1 Mice

Bacterial artificial chromosome (BAC) technology was used to insert a fragment of the human chromosome encompassing the E373A mutated copy of the *DDX58* gene to generate transgenic C57BL/6 mice (Institute of Immunology. Co. LTD.). Transgenic offspring were confirmed by DNA sequencing and founder lines were identified by genotyping PCR of tail DNA using ExTaq enzyme (Takara) with the following primers: forward 5′-CCAGGTATAGAGTTACAGGC-3′, reverse: 5′-ACACAGTGTATGGCACATGG-3′. Lines were maintained as heterozygotes on a C57BL/6 background throughout the study. All mice were housed under specific pathogen-free conditions in the mouse facility. *Mavs*$^{-/-}$ mice were kindly provided by S. Akira (Osaka University), *Ifnar1*$^{-/-}$ and *Rag2*$^{-/-}$ mice were purchased from B&K Universal, and *Il17a*$^{-/-}$ mice were generously provided by Professor Y. Iwakura (Tokyo University of Science). All animal experiments were conducted in compliance with regulations approved by the Committee for Animal Experiments of the Institute for Virus Research, Kyoto University.

2.2 Histology and Immunohistochemistry

Fresh skin tissues were fixed in 10% formalin or 4% paraformaldehyde phosphate (Nacalai Tesque) and embedded in either paraffin or O.C.T compound (Sakura). Five-micrometer cryosections were prepared using a cryotome (Leica CM 3050S). For hematoxylin and eosin (HE) staining, paraffin-embedded slices were stained with hematoxylin and eosin (Funakoshi). Histological analysis was conducted using a BZ-8000 microscope (KEYENCE). Epidermal thickness was considered as the average of 10 measurements of the distance from the basal layer to the stratum corneum using BZ-H1A software (KEYENCE) on all parts of the sectioned tissue. For immunohistochemistry, sectioned tissues were incubated in blocking buffer (10% donkey serum in 0.5% Triton X-100) at room temperature for 1 hour, rinsed in phosphate-buffered saline

(PBS), and stained with anti-CD4 Ab (#25475, Abcam), anti-CD8 Ab (#25478, Abcam), anti-Gr-1 Ab (#108417, Biolegend), anti-CD11c Ab (# 557401, BDbiosciences), anti-cytokeratin-5 ab (#52635, Abcam) and anti-RORγt (#207082, Abcam) at 4°C overnight. Slices were rinsed in PBS and incubated in fluorochrome-conjugated secondary antibody (#711-546-152, Jackson immune research) with DAPI at room temperature for 1 hour. They were then rinsed with PBS, mounted with fluoromount G (Southern Biotech) and examined by confocal microscopy (Leica, TCS SP8).

2.3 Real-time quantitative PCR

Total RNA from homogenized skin tissue was extracted using TRIzol reagent (Invitrogen, Life Technologies) and reverse transcribed using the High-Capacity cDNA Reverse Transcription Kit (Applied Biosystems) with 200 ng of total RNA. Gene expression levels were measured by the StepOnePlus Real-Time PCR system (Applied Biosystems) using TaqMan Fast Universal PCR Master Mix (Applied Biosystems) or Thunderbird SYBR qPCR mix (Toyobo). All quantification cycle data were normalized to *Gapdh* and fold changes were calculated by the ΔΔ Ct method. The TaqMan probes for human and mouse *RIG-I, Ifnb1, Isg56* and *18s* ribosomal RNA were purchased from Applied Biosystems. The primers for SYBR Green Real-Time PCR are listed in Table 1.

2.4 Antibiotic treatment

Mice were treated with broad spectrum antibiotics consisting of 1000 mg of metronidazole (Shionogi), 150 mg enrofloxacin (Bayer Yakuhin), 1000 mg ampicillin (Nacalai Tesque) and 1000 mg kanamycin (Nacalai Tesque) in autoclaved drinking water. Mice were treated from the age of 3 weeks until the age of 30 weeks.

2.5 Tofacitinib treatment

Mice were orally administered 0.5 mg/mouse of CP 690550 citrate (tofacitinib) (TOCRIS bioscience) dissolved in 0.5% methylcellulose (Wako) /0.025% Tween 20 (Nacalai Tesque) 3

times a week. Control mice were orally administered 0.5% methylcellulose and 0.025% Tween 20 solution.

2.6 Flow cytometry and cell sorting

Spleens were harvested and minced, and then treated with 1x RBC lysis buffer (#420301, Biolegend), washed with D-PBS (14249-95, Nacalai Tesque) and subsequently sorted using a cell strainer (Greiner Bio-One) to make cell suspensions. Splenocytes were stained with the following antibodies: FITC-conjugated anti-CD86 (#105006, Biolegend), PE-conjugated anti-CD11c (#557401, BD Pharmingen), APC-conjugated anti-CD45R/B220 (#561880, BD Pharmingen), FITC-conjugated anti-CD44 (#561859, BD Pharmingen), PE-conjugated anti-CD62L (#104408, Biolegend), PerCP-conjugated anti-CD4 (#103234, Biolegend), APC-conjugated anti-CD8 (#553035, BD Pharmingen), FITC-conjugated anti-CD69 (#561929, BD Pharmingen), PE-conjugated anti-CD3E (#100308, Biolegend), PE-conjugated anti-CD11b (#101207, Biolegend), APC-conjugated anti-F4/80 (#123116, Biolegend), APC-conjugated anti-Ly6G (#127614, Biolegend) and APC-conjugated anti-CD19 (#115512, Biolegend). Cells were incubated with antibodies for 20 minutes and washed 3 times with ice-cold PBS. Data were acquired on FACSVerseTM (BD Biosciences) and analyzed with FlowJo software (Tomy Digital Biology).

2.7 Magnetic-Activated Cell Separation (MACS)

A single-cell suspension of spleen cells was prepared as described above, then incubated on ice for 15 minutes with magnetic microbeads for positive isolation, then washed with D-PBS (14249-95, Nacalai Tesque) mixed with 10% FBS (26140087, Gibco, Thermo Fisher Scientific) and centrifuged. Supernatant was discarded and pellet was re-suspended in FACS buffer, washed again and passed through a magnetic cell-sorting column (Miltenyi Biotec). Magnetic microbeads used were CD11c MicroBeads (#130-052-001, Miltenyi Biotec), CD3E MicroBeads (#130-094-

973, Miltenyi Biotec) and CD19 MicroBeads (#130-121-301, Miltenyi Biotec). RNA was purified using RNeasy Micro Kit (#74004, Qiagen), then gene expression levels were measured as described above.

2.8 **Generation of bone marrow-derived dendritic cells (BMDC)**

Bone marrow cells were isolated from the femurs and tibias of mice, treated with RBC lysis buffer, and then cultured in RPMI 1640 (Nacalai Tesque), containing 10% heat-inactivated FBS (Gibco), 50 mM 2-ME, 50 U/ml penicillin/streptomycin, 1 mM sodium pyruvate, 2 mM L-glutamine, and 20 ng/mL recombinant mouse GM-CSF (R&D Systems). A total of 2x105 cells/ml was cultured in 10 ml in petri dish. Half of the media was changed on day 3, and nonadherent cells were collected on day 6.

2.9 Generation of bone marrow-derived macrophage (BMM)

For in vitro BMM differentiation, bone marrow cells were suspended in culture medium [α-MEM (Nacalai Tesque) containing 50 U/ml penicillin/streptomycin (Nacalai Tesque) and 10% heat-inactivated FBS (Gibco)] supplemented with 10 ng /ml of recombinant mouse M-CSF (R&D Systems). A total of 2x106 cells/ml was cultured in 10 ml in petri dish. After culturing for 3 days, floating cells were gently removed by rinsing with PBS, and adherent cells were collected.

2.10 Statistical analysis

Statistical analysis was performed using GraphPadPrism version 8.2.0. Two group-comparisons were performed using unpaired two-tailed Student's t-tests. Data are expressed as means ± SEM except when otherwise indicated and differences are assessed as ns = not significant, *p < 0.05; **p < 0.01, or ***p <0.001. analysis (*p <0.05, **p <0.01, ***p <0.001, ****p <0.0001).

Chapter 3

RESULTS

3.1 hR E373A Tg mice spontaneously developed skin lesion and signs of systemic inflammation.

First, our laboratory generated hR E373A transgenic (Tg) mice expressing the human RIG-I E373A found in SMS patients and I monitored the mice (23). Within the age of 1 year, I found that around one third of hR E373A Tg mice spontaneously developed skin lesion in different parts of their bodies, mostly in the back and tail. This lesion looked red, erosive sometimes covered with white scales (Fig. 1A). The incidence of skin lesion was significantly higher in males than females (Fig. 1B) and the mean onset age in males was 14.37 weeks, which is significantly earlier than females of mean onset age 26.5 weeks. (Fig. 1C). I have also found that the skin lesion was accompanied by signs of systemic inflammation including significant difference in survival rate, which was greater in males than females (Fig. 2A) and growth (Fig. 2B) when compared to the control mice, and major organs showed upregulation of *Isg56* and *Ifnb1* gene expression (Fig. 2C). To determine which cell types are primarily activated to produce type I interferon, I performed cell separation for hR E373A Tg mice spleen and bone marrow differentiation assay for macrophages and dendritic cells, then measured the expression of *Ifnb1* by quantitative RT-PCR, and found that only splenic $CD11c^+$ cells expressed *Ifnb1* upregulation, but not $CD3^+$ cells, $CD19^+$ cells or dendritic cells and macrophages derived from bone marrow cells (Fig. 2D), suggesting dendritic cells as a possible primary source of Ifnb1.

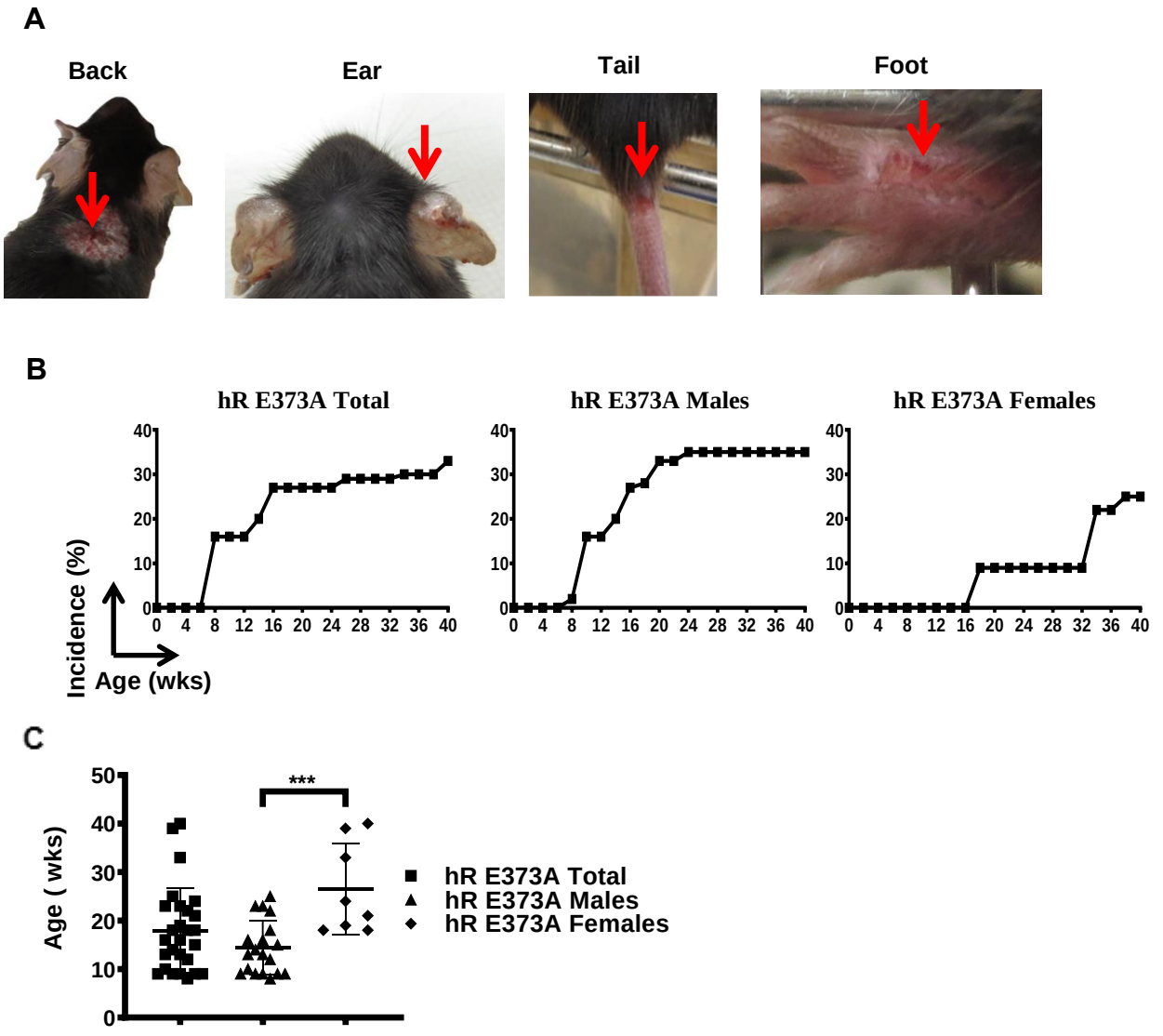

Figure 1: hR E373A mice developed skin lesion

*(A) Images of typical skin lesions of hR E373A Tg mice (red arrows) at different sites, including the back, ear, tail and foot. (B) Incidence rate of skin lesions in all hR E373A Tg mice (n=66), male mice (n=44) and female mice (n=22). (C) Onset age of skin lesions in all hR E373A Tg mice (n=27), male mice (n=19) and female mice (n=8). Student's t-test was used for statistical analysis (***p<0.001).*

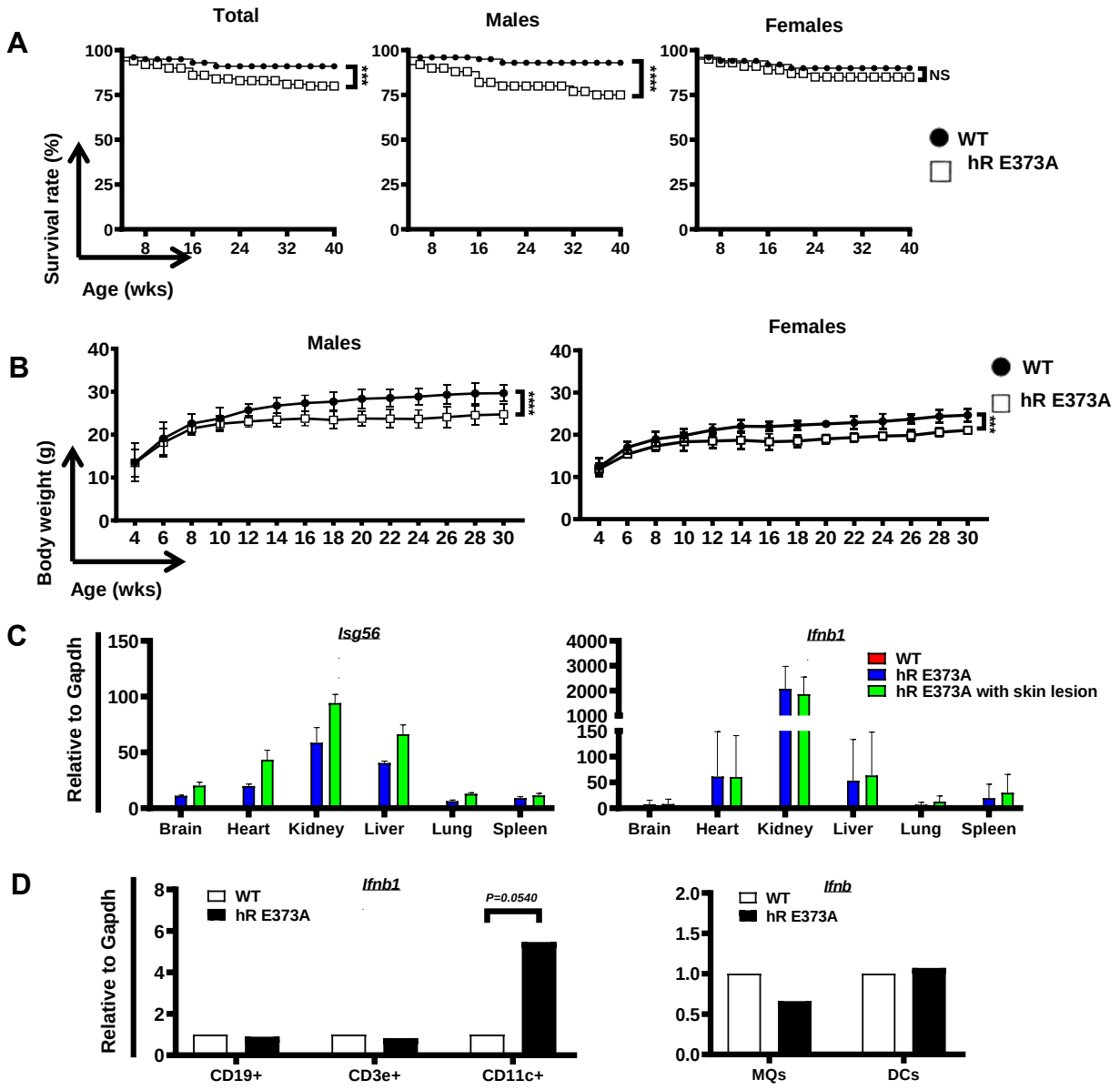

Figure 2: hR E373A mice developed sign of systemic inflammation

*(A) Survival rate of all hR E373A Tg mice (n=100), male mice (n=52) and female mice (n=48) compared with WT littermates (n=111). (B) Change of body weight (mean ± SD) of male hR E373A Tg mice (n=12) compared with WT littermates (n=10) and female hR E373A Tg mice (n=12) compared with WT littermates (n=5). (C) Representative quantitative RT-PCR data for Isg56 and Ifnb1 gene expression in major organs of hR E373A Tg mice (n=3) with skin lesions compared with hR E373A Tg mice (n=3) without skin lesions and WT littermates (n=3). Data are the mean ± SD. (D) (left) Indicated immune cells were sorted from splenocytes and the Ifnb1 mRNA expression level was determined by quantitative RT-PCR. Data are the mean ± SD of triplicate samples. (Right) Ifnb1 mRNA expression levels in GM-CSF induced macrophages (MQs) and dendritic cells (DCs) expressing WT and hR E373A. Data are the mean ± SD of triplicate samples. Student's t-test was used for statistical analysis (***p<0.001, ****p<0.0001). NS: Not significant.*

Moreover, hR E373A Tg also developed splenomegaly, indicating a systemic inflammatory state (Fig. 3A). When I analyzed spleen cells by flow cytometry, both cDCs ($CD11c^{hi}B220^{lo}$) and pDCs ($CD11c^{int}B220^{hi}$), and macrophages ($CD11b^{hi}F4/80^{int}$) of the hR E373A Tg with skin lesion showed upregulation of the expression of cell surface marker, CD86, (Fig. 3B and C) indicating activation of these innate immune cells. Consistent with systemic inflammation, granulocytes were increased in hR E373A Tg mice with skin lesion compared to the control mice (Fig. 3D). Next, I examined T cells, and found that $CD4^+$ and $CD8^+$ T cells showed upregulation of the activation marker CD69 in hR E373A Tg mice with skin lesion (Fig. 4A), indicating an active state. Effector ($CD44^{hi}CD62L^{lo}$) were increased in hR E373A Tg mice with skin lesion, whereas naive T ($CD44^{lo}CD62L^{hi}$) cells were decreased (Fig. 4B), intimating a humoral immune response. Taken together, the data show that hR E373A Tg mice spontaneously developed inflammatory skin lesion, along with signs of systemic inflammation and innate and humoral immune cells activation.

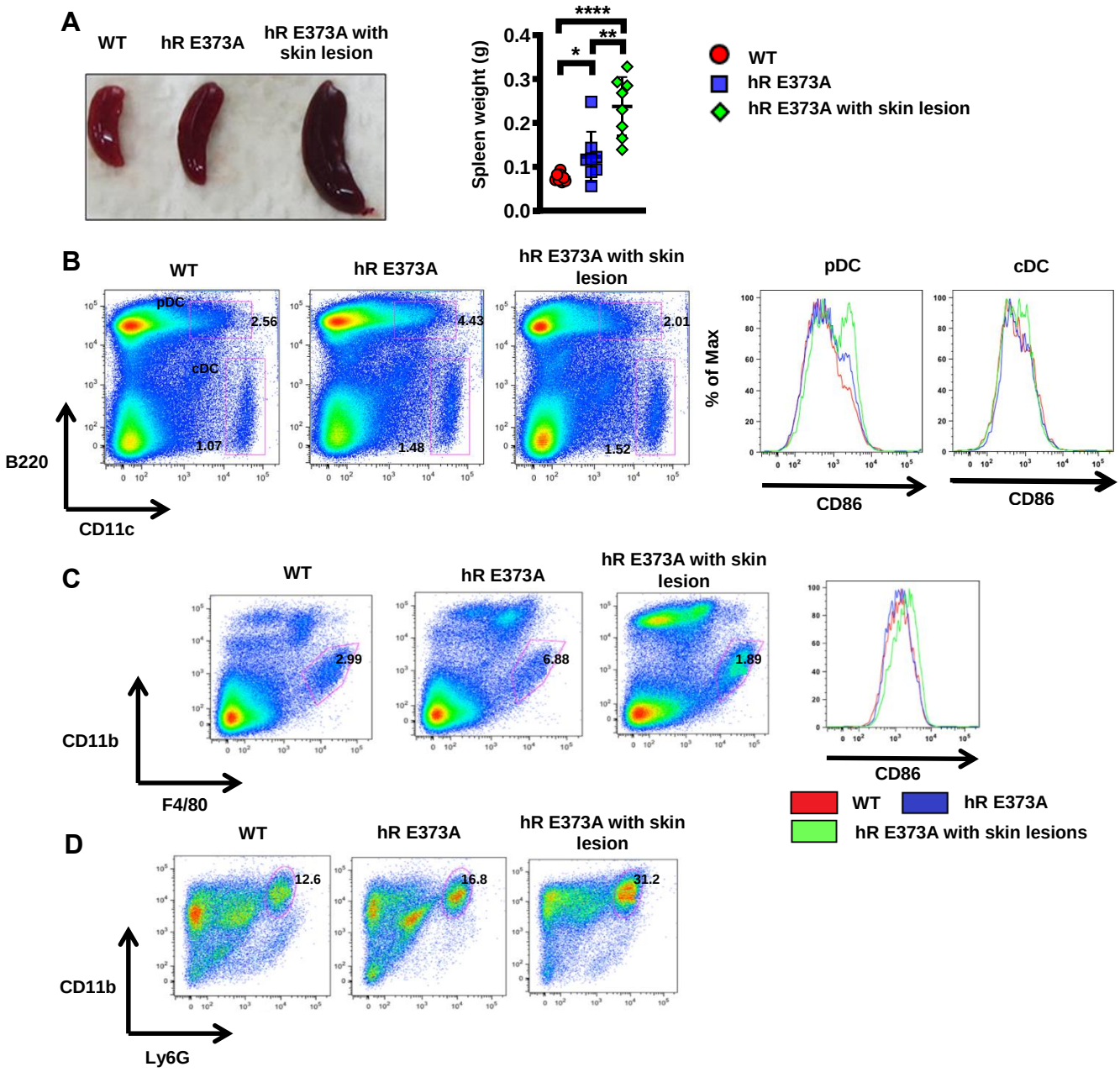

Figure 3: hR E373A mice splenic cells analysis

*(A) Macroscopic image and weight of spleens of hR E373A Tg mice with and without skin lesions compared with those of WT mice (n=8). Data are the mean ± SD. Student's t-test was used for statistical analysis (*p<0.05, **p<0.01, ****p<0.0001). (B) Representative data of FACS analysis of dendritic cells. Splenocytes were stained with CD11c and B220 after MACS depletion of $CD3^+$ and $CD19^+$ cells, then pDC and cDC were isolated for the analysis of CD86 expression. (C) Representative data of FACS analysis of macrophages cells. Splenocytes were stained with CD11b and F4/80 after MACS depletion of $CD3^+$ and $CD19^+$ cells, then isolated for the analysis of CD86 expression. (D) Representative data of FACS analysis of splenic neutrophils expression of CD11b and Ly6G.*

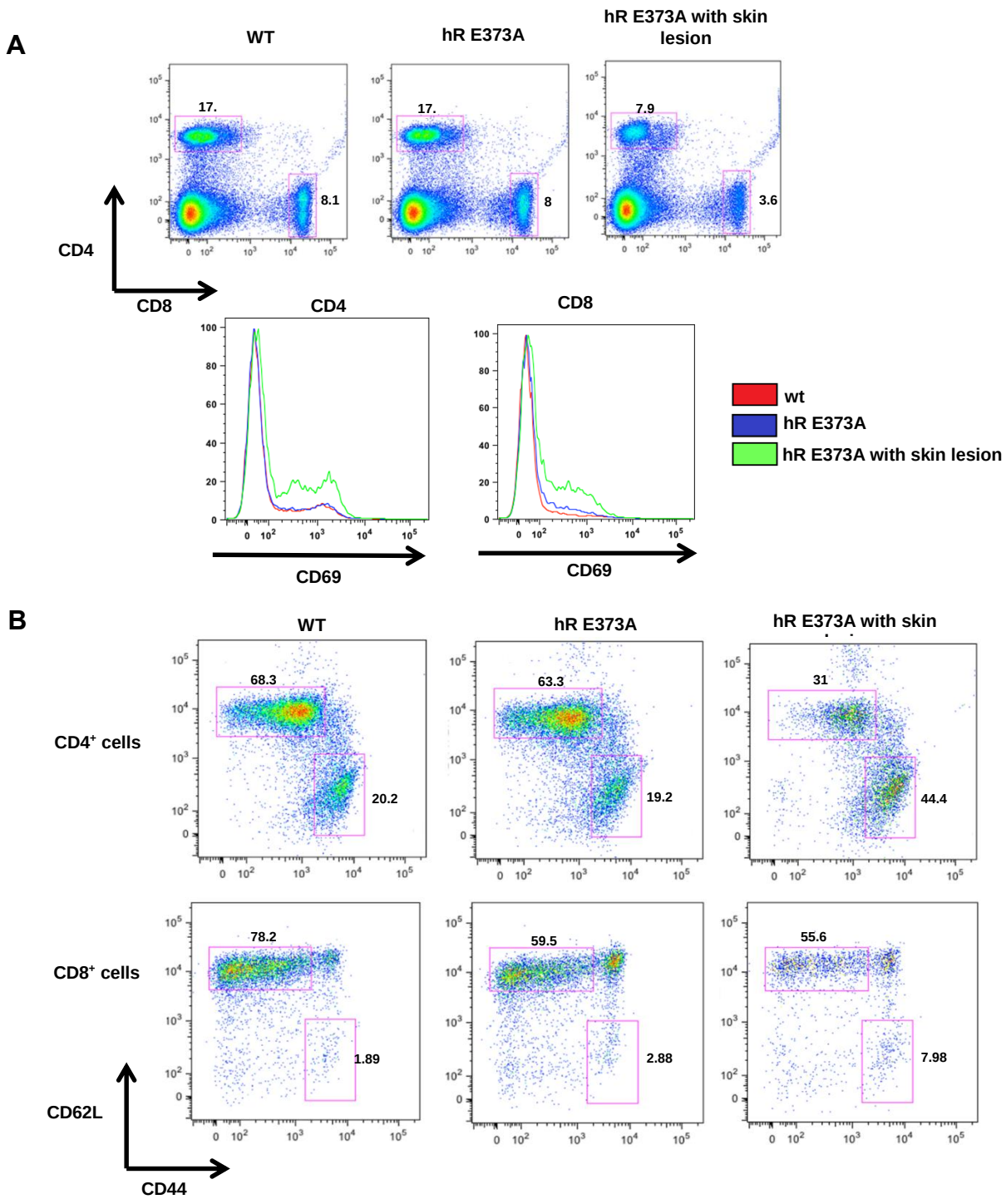

Figure 4: hR E373A mice splenic T cells analysis

(A) Representative data of FACS analysis of splenicT cells. Splenocytes were stained with CD4 and CD8 and further analyzed for the expression of CD69. (B) Representative data of FACS analysis of T-cells. CD4 and CD8 cells were isolated from the spleen (n=3), and further analyzed for the expression of CD44 and CD62L.

3.2 Histological analysis and cytokines expression profile of the skin lesion of hR E373A Tg mice show similarities with human psoriasis.

Next, I wanted to identify the histological features of the lesion, so I performed Hematoxylin and eosin (H&E) of the affected and control skin. Histological analysis of the affected skin showed typical histological findings to psoriasis, including a significant increase in the epidermal thickness, termed acanthosis, retention of keratinocyte nuclei in the stratum corneum (parakeratosis), thickening of the stratum corneum (hyperkeratosis) and sometimes rete-like elongations deep into the dermis, accompanied with infiltrates of inflammatory cells in the epidermis and dermis (Fig. 5A and B), which are all consistent with skin psoriasis. Basal proliferating layer of epidermis and suprabasal layer of the affected skin stained more with keratin 5 compared to the wild type control, indicating promoted keratinocytes differentiation and proliferation in the skin lesion of hR E373A Tg mice (Fig. 5C). Furthermore, immunohistochemistry of the affected skin showed abundant leukocytes including $CD11c^+$ and $Gr\text{-}1^+$ cells in the dermis and epidermis compared with wt control (Fig. 5D), Moreover, $CD4^+$ and $CD8^+$ cells were also detected in the skin lesion of hR E373A Tg mice (Fig. 5D), indicating infiltrates of neutrophils, dendritic cells and T cells.

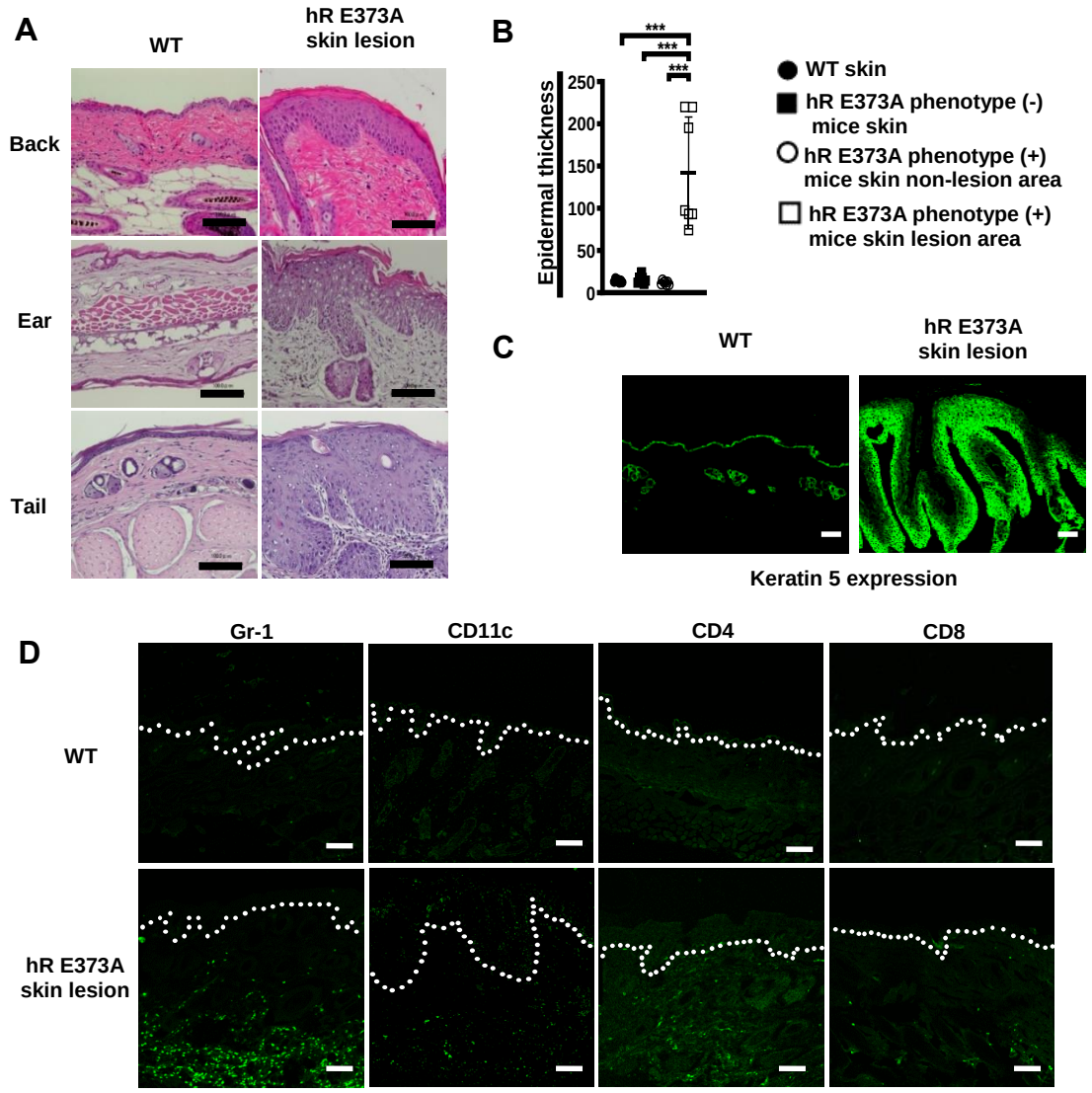

Figure 5: Histological analysis of hR E373A mice skin lesion area

(*A) Representative HE staining of skin lesions on the back, ear or tail of WT or hR E373A Tg mice (Bar = 100 µm). (B) Epidermal thickness in WT mice (n=7), hR E373A Tg mice without skin phenotype (n=7), non-skin lesion area or skin lesion area in hR E373A Tg mice developing the skin phenotype (n=7). Data are the mean ± SD. (C) Representative immunohistochemistry for keratin 5 in the skin lesions of hR E373A Tg mice and WT littermates. (D) Representative immunohistochemistry of Gr-1, CD11c, CD4 and CD8 in the skin lesions of hR E373A and WT mice (n=3). Student's t-test was used for statistical analysis (***p<0.001). (Bar = 100 µm).*

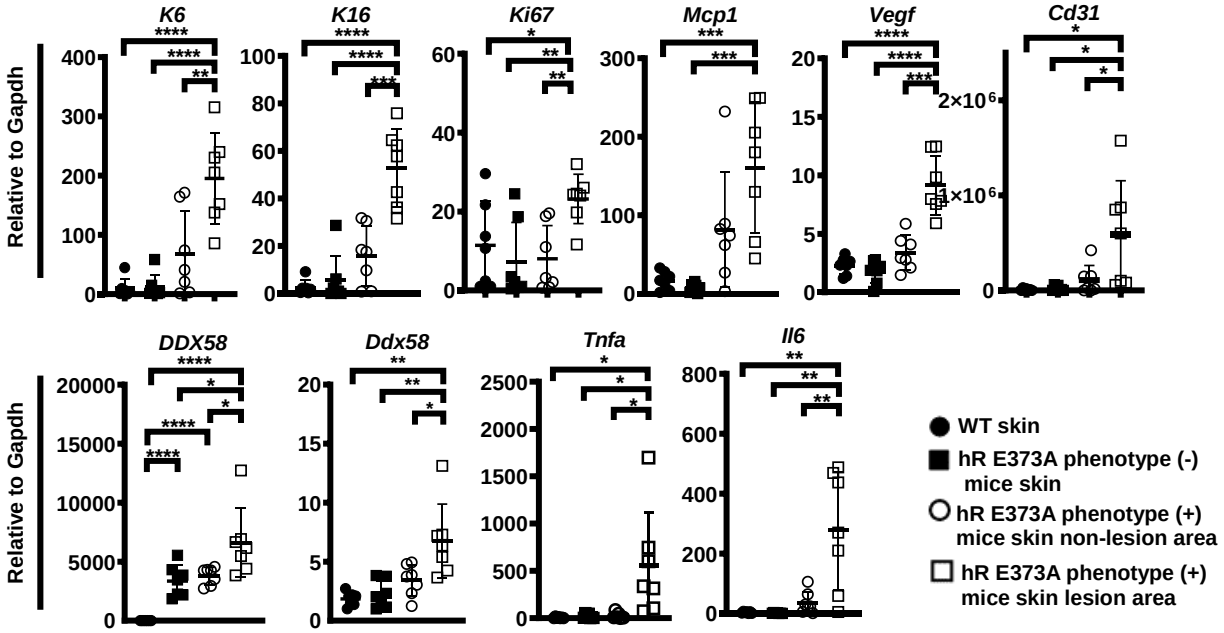

Figure 6: Cytokines profile of hR E373A mice skin lesion area
*Expression of genes by qRT-PCR relative to Gapdh gene expression and normalized to WT skin. Data are the mean ± SD. Student's t-test was used for statistical analysis (*p<0.05, **p<0.01, ***p<0.001, ****p<0.0001).*

qRT PCR assessment of hyperproliferation markers of keratinocytes, *K6, K16* and *Ki67* showed significant upregulation as well as significantly high expression of angiogenesis markers such as monocyte chemoattractant protein-1 (*Mcp1*), vascular endothelial growth factor (*Vegf*) and *Cd31* genes in the skin lesion of hR E373A Tg mice (Fig. 6). In this transgenic mice, the expression of the gene *Ddx58* that encodes RIG-I was significantly increased in the affected skin compared with the non-lesion or wt controls (Fig. 6). Consistent with that, cytokines related with RIG-I downstream signaling such as *Tnfa* and *Il6* genes were also upregulated (Fig. 6). Collectively, histological features of the skin lesion of hR E373A Tg mice resemble typical psoriatic skin with upregulated expressions of RIG-I and its downstream cytokines, indicating potential involvement of RIG-I for the pathogenesis of inflammatory skin lesion.

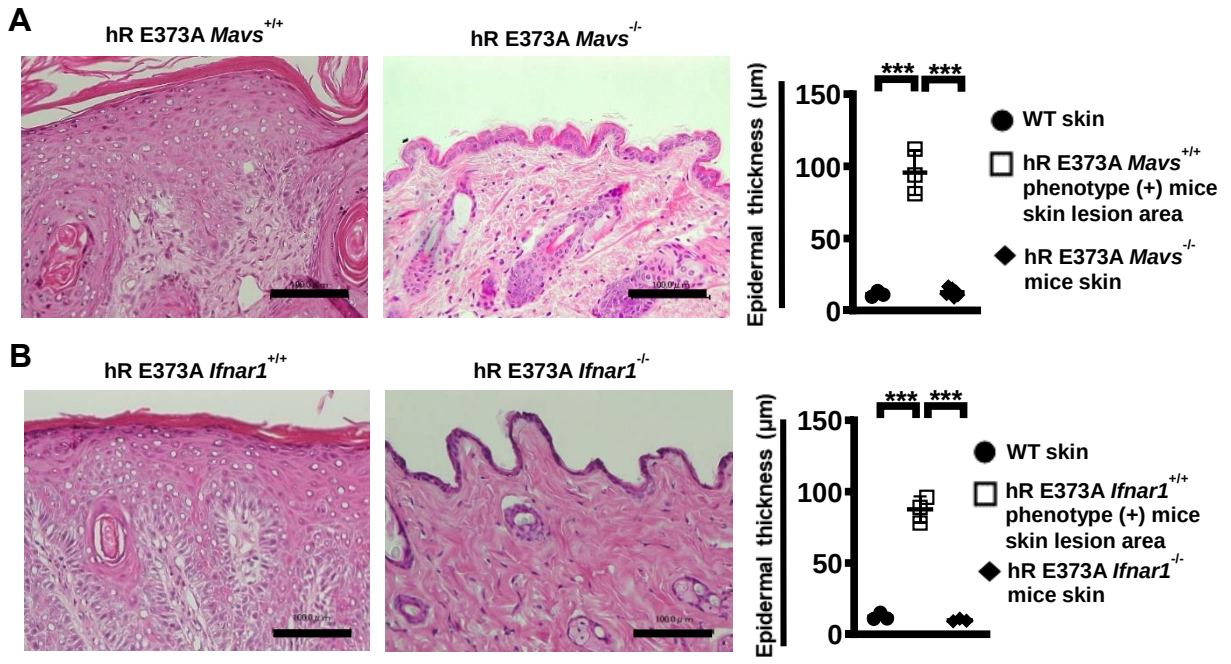

Figure 7: hR E373A Mavs$^{-/-}$ and hR E373A Ifnar1$^{-/-}$ mice showed normal skin
*(A) Left: Representative HE staining of the back of skin lesions in hR E373A Mavs$^{+/+}$ mice and hR E373A Mavs$^{-/-}$ mice (n=3) Right: Epidermal thickness of WT (n=3), and skin lesions of hR E373A Mavs$^{+/+}$ (n=3) and hR E373A Mavs$^{-/-}$ mice (n=7). Data are the mean ± SD. (B) Left: Representative HE staining of skin lesions on the back in hR E373A Ifnar1$^{+/+}$ mice and hR E373A Ifnar1$^{-/-}$ mice (n=3) (bar=100 μm). Right: Epidermal thickness in WT (n=3), skin lesion of hR E373A Ifnar1$^{+/+}$ (n=3) and hR E373A Ifnar1$^{-/-}$ mice (n=3). Data are the mean ± SD. Student's t-test was used for statistical analysis (***p<0.001). (bar=100 μm)*

RIG-I signaling pathway involves the utilization of Mitochondrial antiviral-signaling protein (MAVS) for the type I IFN-mediated antiviral immune response (25). To further elucidate the involvement of RIG-I in the pathogenesis, I intercrossed the transgenic mice with *Mavs*$^{-/-}$ mice or *Ifnar1*$^{-/-}$ mice. The transgenic mice deficient in both genes resulted in absence of the skin lesion with normal histological manifestations (Fig. 7A and B). Collectively, histological features of the skin lesion of hR E373A Tg mice resembled typical psoriasis with upregulated expression of RIG-I and its downstream cytokines, which was cancelled by deficiency of MAVS or IFNAR1, directly indicating involvement of RIG-I for the pathogenesis of psoriasis-like skin lesion.

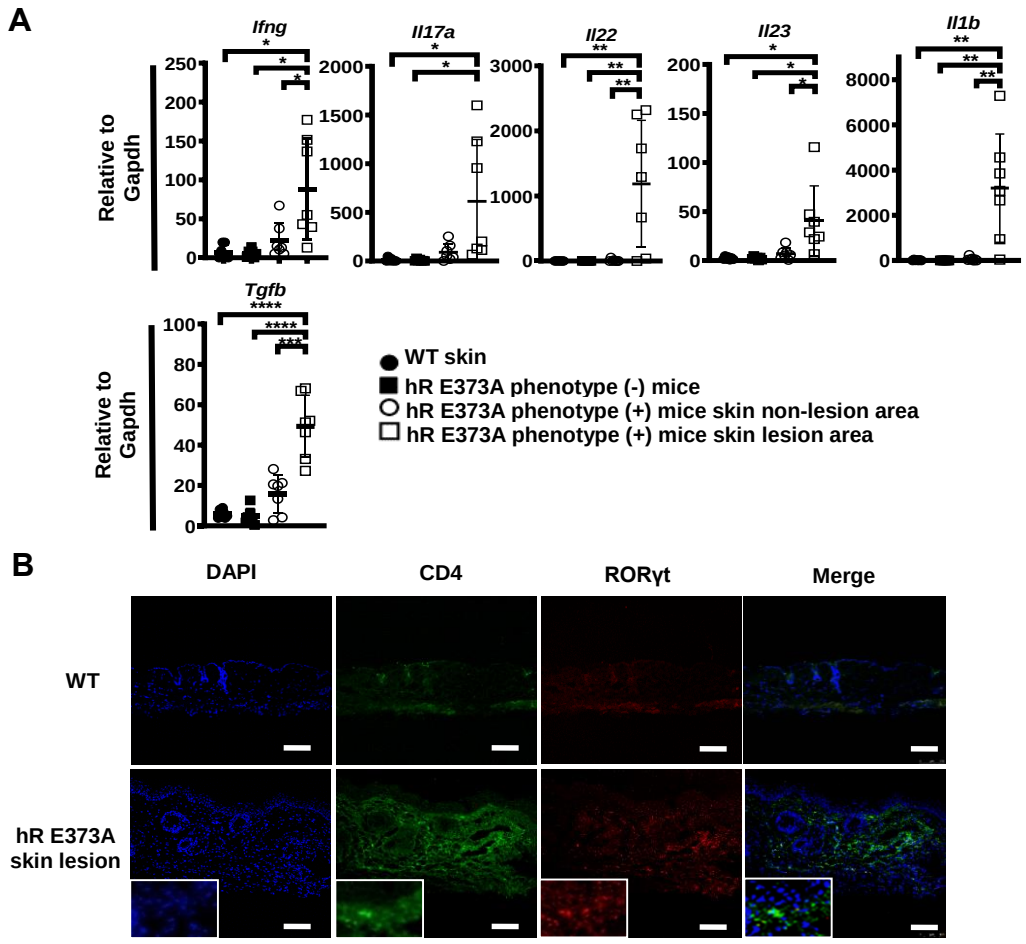

Figure 8: Th17 cytokines hR E373A mice skin lesion area

*(A) Quantitative RT-PCR of indicated genes relative to Gapdh gene expression and normalized to WT skin. Data are the mean ± SD. (B) Representative immunohistochemistry of DAPI (blue), CD4 (green) and RORγt (red) in the skin lesions of hR E373A and WT mice (n=3). Data are the mean ± SD. Student's t-test was used for statistical analysis (*p<0.05, **p<0.01, ***p<0.001, ****p<0.0001). (bar=100 µm).*

3.3 Il-23/Il-17 axis is involved in the pathogenesis of the skin lesion of hR E373A Tg mice.

IL-23/IL-17 axis have been reported to play a central role in the development of skin psoriasis (26). Consistent with the reports implicating Th1 cells and Th17 cells in the development of skin psoriasis in human and mouse model (27-29), hR E373A Tg mice qRT-PCR analysis of the inflamed skin showed significant expression of *Ifng* and *Il17a*, as well as other IL-23/IL17 axis cytokines such as *Il22* and *Il23*, while *Il1b* and *Tgfb*, which do promote Th17 differentiation were

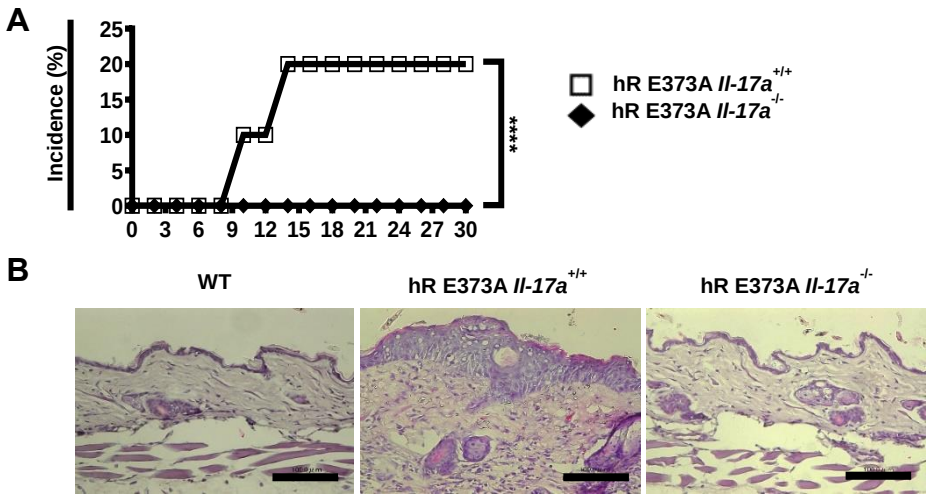

Figure 9: hR E373A Il17$^{-/-}$ mice skin incidence and histological analysis
*Incidence of skin lesions in hR E373A Il17a-/- mice (n=14) and hR E373A Il17a+/+ littermates (n=9). (B) Representative HE staining of skin lesion on the back of hR E373A Il17a -/- mice compared with hR E373A Il17a +/+ and WT mice (bar=100 µm). Student's t-test was used for statistical analysis (****p<0.0001). (bar=100 µm).*

also significantly expressed (Fig. 8A). Retinoic Acid Receptor-Related Orphan Receptor γt (RORγt) is a transcriptional factor that has been shown to play an important role in Th17 differentiation from naïve CD4 cells (30, 31). In accordance with that, immunohistochemistry of the diseased skin revealed infiltrates of $CD4^+$ cells coexpressing with RORγt (Fig. 8B). Taken together, results show that the skin lesion confers Th17 signature, indicating a central role for IL-23/IL-17 axis in the pathogenesis of the skin phenotype. To further check the involvement of IL-17A in the development of the skin lesion, I generated hR E373A *Il17a*$^{-/-}$ transgenic mice and monitored the phenotype. As shown in Fig.9, hR E373A *Il17a*$^{-/-}$ mice showed no skin phenotype compared to hR E373A *Il17a*$^{+/+}$ mice (Fig. 9A), while histological analysis revealed normal skin (Fig. 9B), suggesting that IL-17A is essential in the development of the skin lesion. In conclusion, the data shows that the skin lesion in this transgenic mice shows induction of Th17 cytokines, and that IL-17A deficiency protected the mice from developing the psoriasis-like skin lesion.

3.4 Mature lymphocytes are involved in the development of skin lesion in hR E373A Tg mice

In order to check the role of mature lymphocytes in the development of psoriasis-like skin lesion, I generated hR E373A *Rag2*$^{-/-}$ mice (which lack mature lymphocytes) and observed the skin phenotype. As shown in Figure 10A, the incidence of inflammatory skin lesion development was significantly lower in hR E373A *Rag2*$^{-/-}$ mice compared to hR E373A *Rag2*$^{+/+}$, though the average onset age was almost the same (Fig. 10B). However, the lesion in hR E373A *Rag2*$^{-/-}$ mice looked milder, i.e., smaller in size and less erosive than that of hR E373A *Rag2*$^{+/+}$ mice (Fig. 10C).

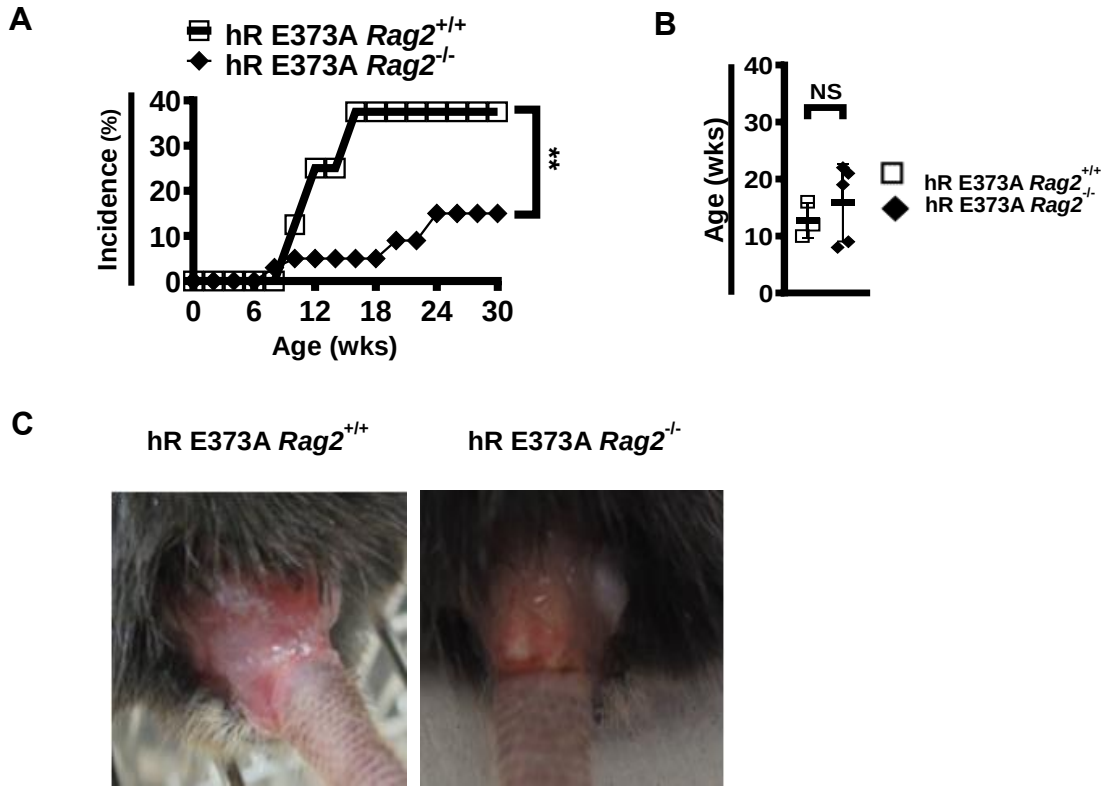

Figure 10: hR E373A Rag2$^{-/-}$ phenotype (+) mice skin lesion incidence and appearance
*(A) Incidence of skin lesions in hR E373A Rag2$^{-/-}$ mice (n=33) and hR E373A Rag2$^{+/+}$ littermates (n=8). (B) Age of onset of skin lesions in hR E373A Rag2$^{-/-}$ mice (n=5) compared with hR E373A Rag2$^{+/+}$ mice (n=3). (C) Macroscopic images of skin lesions of hR E373A Rag2$^{+/+}$ and hR E373A Rag2$^{-/-}$ mice. Student's t-test was used for statistical analysis (**p<0.01). NS: Not significant.*

When I analyzed the lesion histologically, I found that psoriatic features such as hyperkeratosis, acanthosis and parakeratosis were apparently improved in the skin lesion of hR E373A *Rag2*$^{-/-}$ mice (Fig. 11A), which is further confirmed by less keratin 5 expression in the lesion (Fig. 11B). Immunohistochemistry revealed some expression of Gr-1^{+} cells and CD11c^{+} cells in the dermis and epidermis in hRE373A *Rag2*$^{-/-}$ (Fig. 11C), however, their mRNA expression was decreased when compared with hR E373A *Rag2*$^{+/+}$ mice (Fig. 11D).

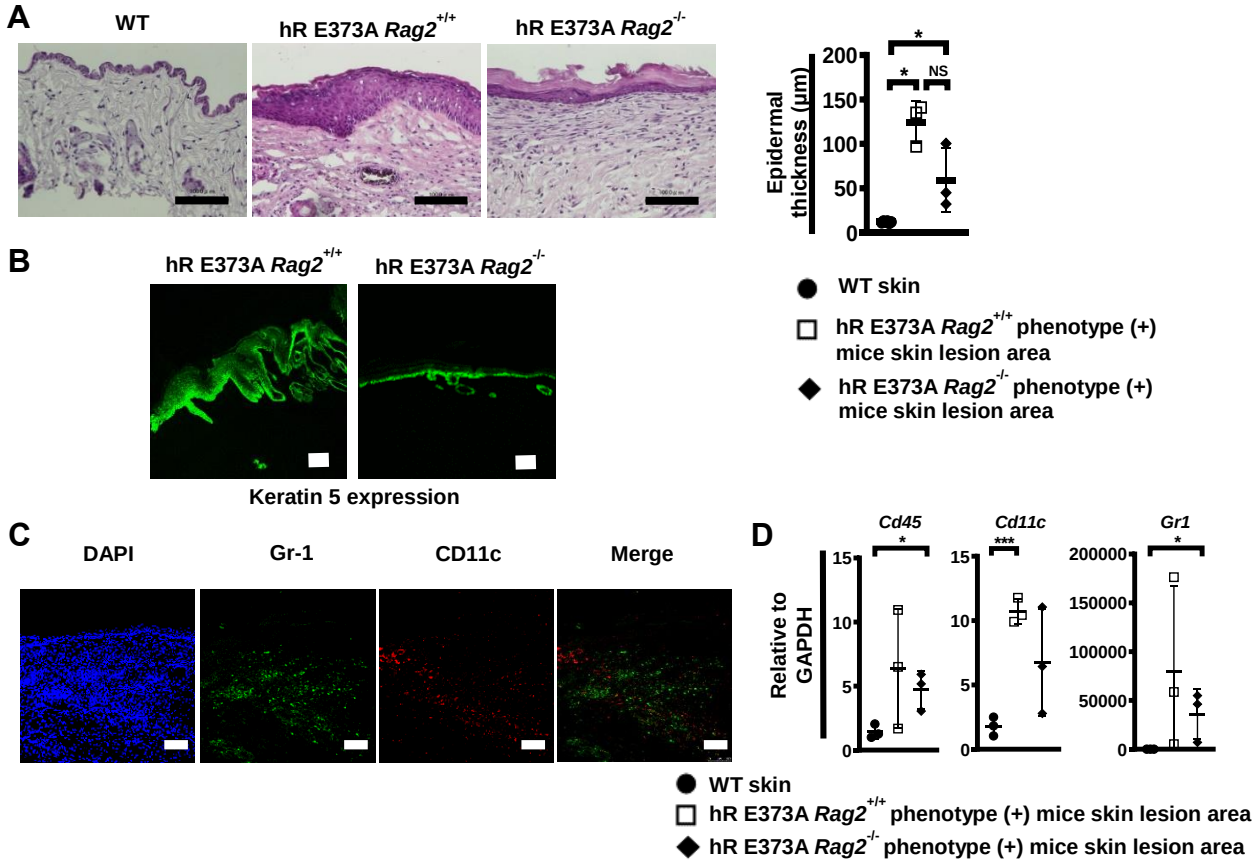

Figure 11: hR E373A Rag2$^{-/-}$ phenotype (+) mice skin histological analysis
*(A) Representative HE staining of skin lesions (left, bar=100 µm) Epidermal thickness (right) in hR E373A Rag2$^{-/-}$ skin lesion (n=3) compared with hR E373A Rag2$^{+/+}$ skin lesion (n=3) and WT (n=6). (B) Representative immunohistochemistry of skin lesion of hR E373A Rag2$^{-/-}$ and WT littermate stained for keratin 5 (n=3). (C) Representative immunohistochemistry of skin lesions of hR E373A Rag2$^{-/-}$ mice for CD11c and Gr-1. (D) qRT-PCR of indicated genes in hR E373A Rag2$^{-/-}$ (n=3) skin lesion compared with skin lesion of hR E373A Rag2$^{+/+}$ littermates (n=3) and WT littermates (n=3) relative to Gapdh and normalized to WT skin. Data are the mean ± SD. Student's t-test was used for statistical analysis (*p<0.05, ***p<0.001). (bar=100 µm).*

qRT PCR analysis showed a clear decrease in the expression of *K6* and *K16*, as well as proangiogenesis markers *Mcp1* and *Vegf* (Fig. 12A). The expression of inflammatory cytokines such as *Il17a, Tnfa, Il1b* and *Il6* was also downregulated in hR E373A *Rag2*$^{-/-}$ mice (Fig. 12B) suggesting that the production of IL-17A and TNF-α, which are key cytokines for psoriasis, was largely dependent on T cells. On the other hand, *Il22* and *Il23* were still expressed in the skin lesion of hR E373A *Rag2*$^{-/-}$ mice (Fig. 12B) indicating that the production of these cytokines are dependent on nonlymphocid cells. Taken together, the data shows that lymphocytes play an important role in the development of psoriasis-like skin lesion in hR E373A Tg mice, however, their absence did not abrogate the phenotype.

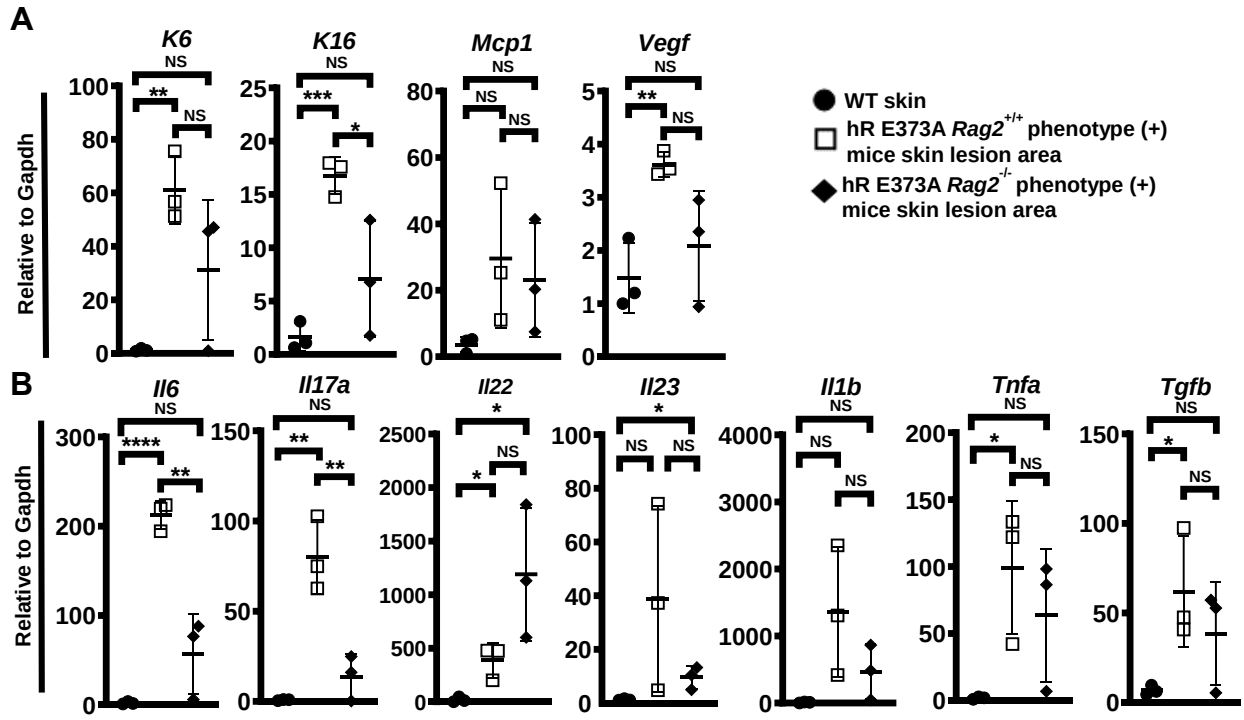

Figure 12: hR E373A Rag2$^{-/-}$ phenotype (+) mice skin cytokines profile
*qRT-PCR of indicated genes in hR E373A Rag2$^{-/-}$ (n=3) skin lesion compared with skin lesion of hR E373A Rag2$^{+/+}$ littermates (n=3) and WT littermates (n=3) relative to Gapdh and normalized to WT skin. Student's t-test was used for statistical analysis (*p<0.05, **p<0.01, ***p<0.001, ****p<0.0001). NS: Not significant*

3.5 Commensal microbiota plays a role in the development of skin lesion in hR E373A Tg mice.

Next, I wanted to check the role of commensal microbiota (CM) in the development of the skin lesion here. Commensal microbiota have been associated with the development of a group of autoimmune diseases, such as rheumatoid arthritis, asthma and type 1 diabetes (32-34). CM have also linked with the development of skin psoriasis (35, 36). It is also reported that gut microbiota is involved in the development of psoriasis by enhancing Th17 response (37). In our model, I treated mice with broad-spectrum antibiotics in autoclaved drinking water from the age of 3 weeks until 20 weeks. Stool minced in PBS and cultured in agar plate showed huge reduction in the CM in antibiotic-treated mice, and the expression of *16s* was almost abolished on the skin (Fig.13A and B). The treatment with antibiotics has decreased the incidence of skin lesion though the onset age was just slightly changed (Fig. 13C and D).

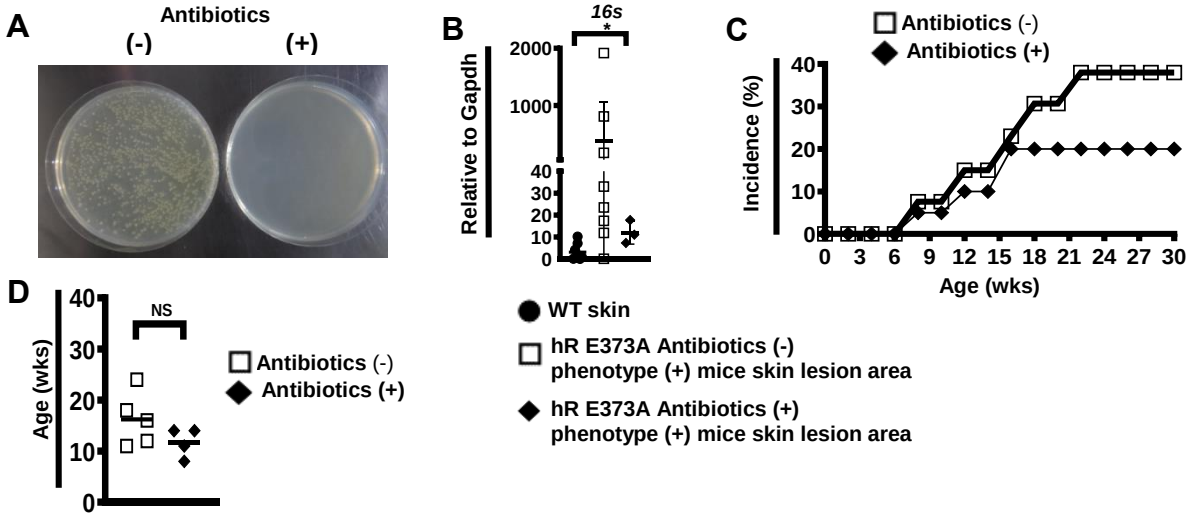

Figure 13: hR E373A antibiotic-treated mice
(A) Clearance of gut bacteria by antibiotic treatment. Feces of control (-) and antibiotic-treated hR E373A mice were examined for gut microbiota by agar plate culture. (B) Expression of the 16s gene in the antibiotic-treated or non-treated skin of hR E373 mice. (C) Incidence of skin lesions in hR E373A Tg mice treated with antibiotics (n=20) and non-treated mice (n=13). (c) Age of onset of skin legion with or without antibiotic treatment. (D) Representative tail skin lesion of control

*and antibiotic-treated mice. Data are the mean ± SD. Student's t-test was used for statistical analysis (*p<0.05). NS: Not significant.*

The skin lesion of antibiotic-treated mice looked less erosive (Fig. 14A), indicating that antibiotics treatment ameliorated the severity of skin phenotype. Histological analysis showed a significant decrease in the epidermal thickness with milder hyperkeratosis, and a complete absence of parakeratosis and rete-like elongations (Fig. 14B). Similarly, the expression of keratin 5 was also decreased in antibiotics-treated hR E373A Tg mice (Fig. 14C). Moreover, analysis of the Th17 axis cytokines showed a downregulation of *Il17a*, as well as *Tnfa*, *Il6*, *Il1b* and *Tgfb* (Fig. 13D) though it is statistically not significant. These results collectively indicate that CM affected the severity of skin lesion through modulating Th17 response.

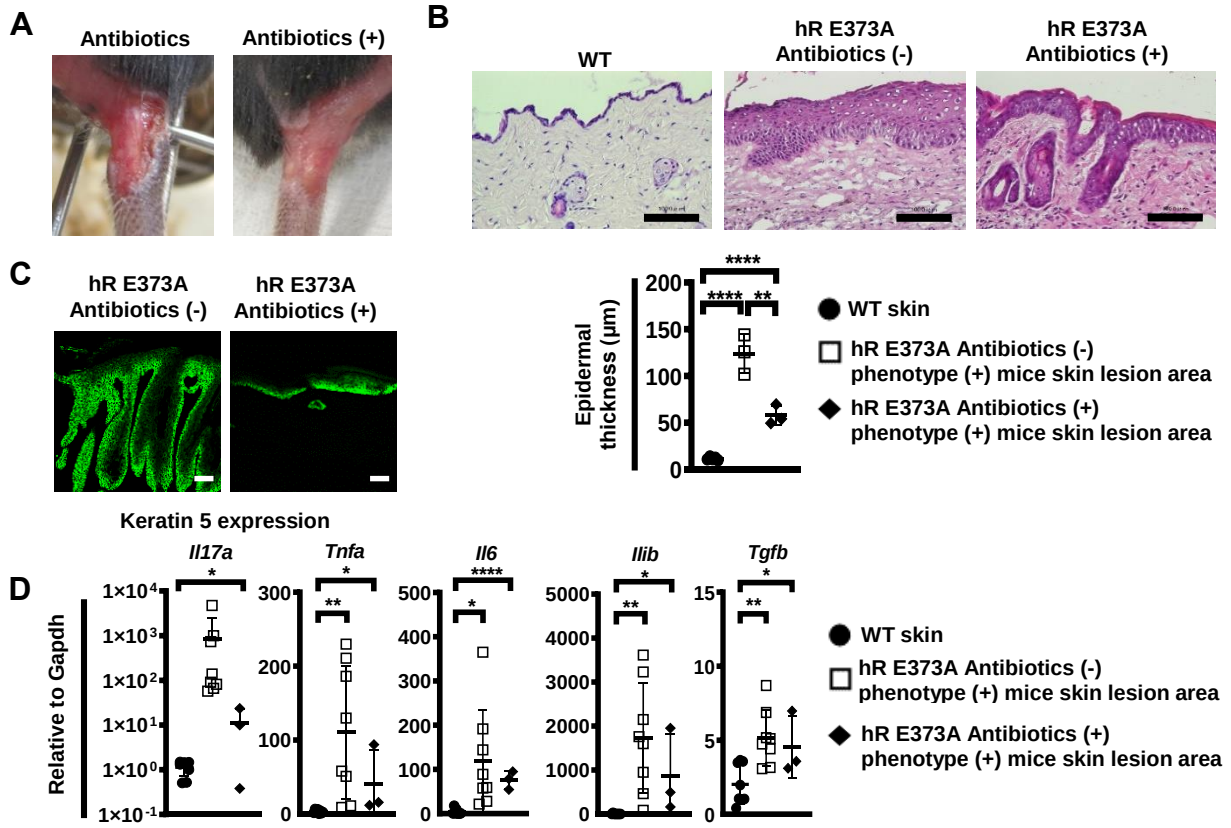

Figure14: hR E373A antibiotic-treated mice skin incidence and histological analysis
(A) Representative tail skin lesion of control and antibiotic-treated mice. (B) Up: Representative HE staining of skin lesions on the back of hR E373A Tg mice treated with antibiotics compared with hR E373A non-treated mice and WT mice (n=3) (left). Down: Epidermal thickness in these

*mice (C) Immunohistochemistry for Keratin 5 expression in antibiotic-treated or non-treated hR E373A mice. (D) Expression of the indicated genes in the antibiotic-treated or non-treated skin of hR E373 mice relative to Gapdh gene expression and normalized to WT skin. Data are the mean ± SD. Student's t-test was used for statistical analysis (*p<0.05, **p<0.01, ***p<0.001, ****p<0.0001). (bar=100 µm).*

3.6 Janus kinase (JAK) inhibitor ameliorated skin phenotype of hR E373A Tg mice

Tofacitinib is a drug that is used to treat moderate to severe rheumatoid arthritis (RA) (38), psoriasis (39), and ulcerative colitis (40) by inhibiting JAK1 and JAK3 (41). This JAK inhibition results in immune response suppression and blockade of signal of type-1 interferon and many other inflammatory cytokines including IL-2, IL-4, IL-7, IL-9, and IL-15 (42). Here, I wanted to validate hR E373A Tg mice as a psoriasis model and to investigate the effect of tofacitinib treatment on the development of the skin lesion, so I treated mice with 0.5 mg tofacitinib orally 3 times a week and monitored the phenotype. Treatment with tofacitinib resulted in complete absence of skin phenotype in hR E373A Tg mice compared to hR E373A Tg mice non-treated mice (Fig. 15A and B). Histological analysis revealed normal skin in the hR E373A Tg treated mice (Fig. 15C). The treatment has also suppressed the activation of T-cells in the spleen of hR E373A Tg mice compared to the non-treated mice (Fig. 14D).

A

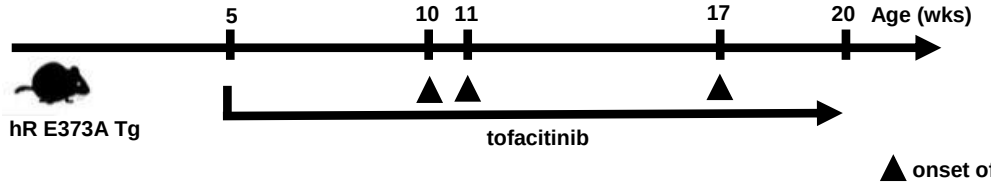

B

	Total number	Number that developed skin lesions	Age of onset (wks)	Incidence (%)
Control	10	3	10, 11, 17	30
Tofacitinib	10	0	-	0

C

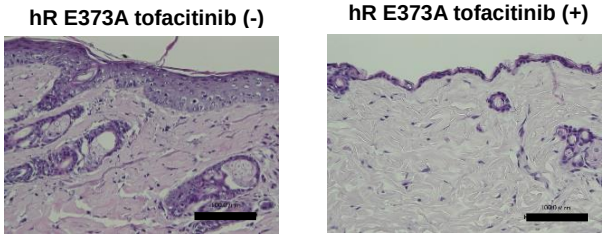

D

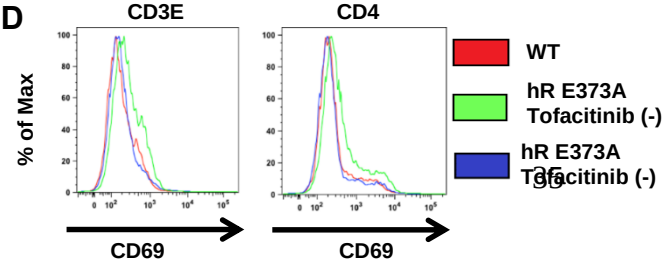

Figure 15: hR E373A Tg mice treated with tofacitinib did not develop skin lesion
(A) Schematic diagram of tofacitinib treatment of hR E373A Tg mice. Mice were orally administered tofacitinib or vehicle control from the age of 5 weeks before the onset of skin lesions to 20 weeks. (B) Summary of skin lesion development during tofactinib treatment. (C) Representative HE staining of skin lesions on the back of hR E373A Tg mice with tofacitinib or control treatment. Bar = 100 µm. (D) Representative FACS analysis of CD69 expression in splenic $CD3E^+$ (left) and $CD4^+$ cells (right) from tofacitinib-treated or non-treated hR E373A Tg mice and WT mice. (bar=100 µm).

Moreover, hR E373A Tg mice with skin lesion that were treated with tofacitinib for 3 weeks have shown improvement of the pathology of skin (Fig. 16). Taken together, the data show that tofacitinib treatment revoked the lesion, and improved the pathology in mice which already developed skin lesion.

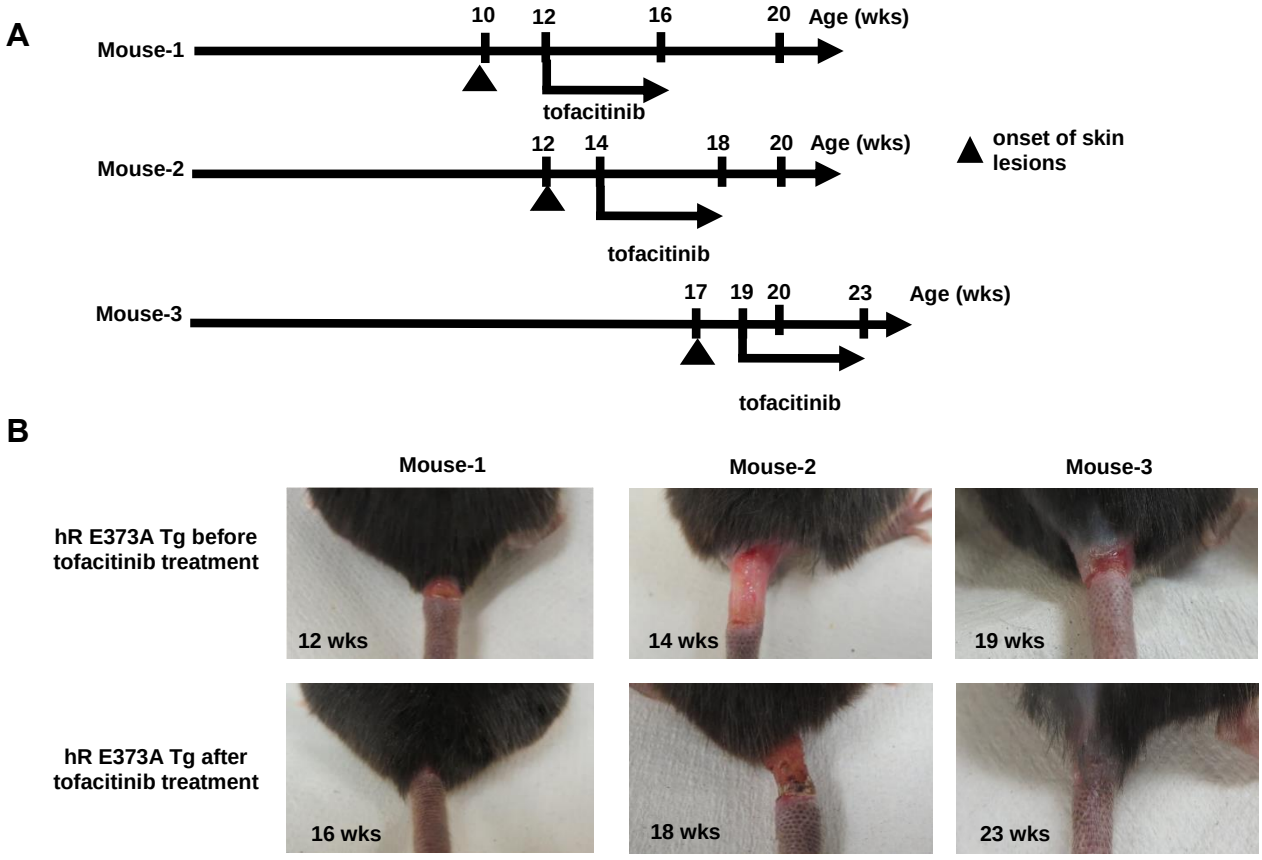

Figure 16: hR E373A Tg mice treated with tofacitinib
(A) Schematic diagram of hR E373A Tg mice treated with tofacitinib for 4 weeks after the development of skin lesions. (B) Skin lesion site of the 3 mice before and after tofactinib treatment.

3.7 hR E373A Tg mice developed other co-morbidities

Skin psoriasis is usually associated with other co-morbidities (43). Around 25% of patients with psoriasis develop psoriatic arthritis (44). In addition to the development of skin lesion in hR E373A Tg mice, I noticed that few of mice had swollen ankle joint. H&E staining of the ankle joint section showed thickening of the synovium with cell infiltrates, and some proliferation of the synovial joint, indicating joint inflammation (Fig. 17). The skin of the inflamed joint showed epidermal thickening and thickening of the stratum corneum (hyperkeratosis) along with cellular infiltration. This is an important finding, however, the link between arthritis and skin psoriasis in our model needs further investigations and analysis.

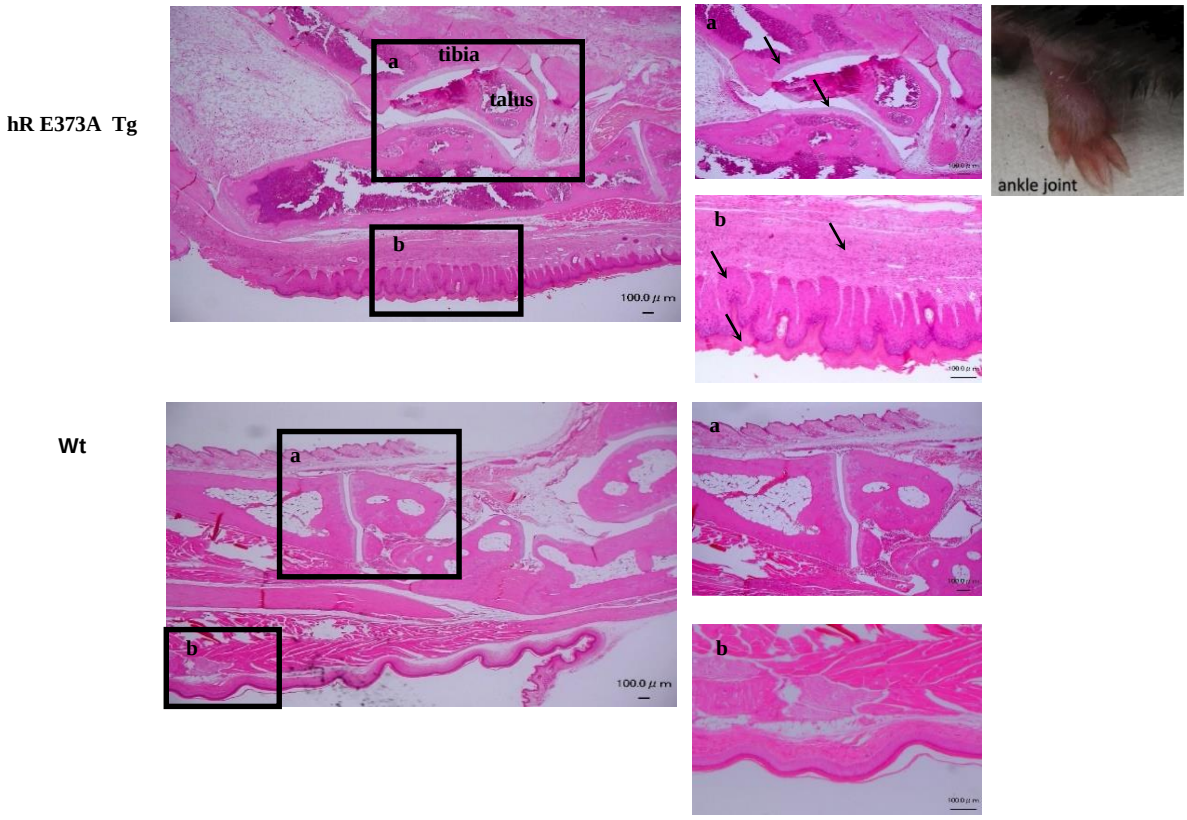

Figure 17: hR E373A Tg mice developed foot co-morbidities
Representative HE staining of ankle joint section of hR E373A Tg mice or control treatment. (bar=100 µm).

Chapter 4

DISCUSSION

Psoriasis is a common chronic inflammatory skin disease affecting 2-3% of the population worldwide (45) with prevalence rates influenced by both genetics and environmental factors (46). It is characterized by abnormal silver-white scaling and erythematous plaques.(47) It is one of the most researched immune-mediated diseases, utilizing many induced mouse models. RIG-I–like receptors (RLR) have been reported to be involved in many autoimmune diseases affecting different organs, including skin. In genome wide association study (GWAS) among psoriasis patients, SNPs in *IFIH1* which encodes MDA5 (48) and in *DDX58* which encodes RIG-I (17) are significantly associated with psoriasis. Recently mutations in *IFIH1* and *DDX58* have been identified in patients with a rare autoimmune disease , SMS, that exhibits interferon signature and develops psoriasis-like skin lesion as one of the symptoms (10, 49-51). Especially in the SMS cases of *DDX58*, two mutations encoding RIG-I E373A and C268F were identified and 7 out of 11 patients were reported to exhibit skin manifestations including psoriasis and atopic dermatitis (50).

In hR E373A Tg mice, interferon signature in multi-organs was observed (Fig. 2C), and only splenic $CD11c^+$ cells expressed *Ifnb1* gene (Fig. 2D), suggesting dendritic cells as a possible primary source of Ifnb1. This could be related to the epigenetic factors controlling RIG-I signaling or other type 1 IFN signaling pathway (52-54).

The rate of skin lesion onset was approximately 33% (Fig. 1b). The incidence of skin lesion was significantly higher in males (35%) than females (25%) within 40 weeks of age (Fig. 1b and 1c). This is similar to the incidence of skin manifestations in patients with atypical SMS where all the 3 males diagnosed with the disease had skin manifestations in comparison to half of the 8 females diagnosed (Mi-Ae Jang *et el*,2015), however, no sex difference was observed in appearance of the lesion, histological characteristics and cytokine profiles (data not shown).

Investigating this sex difference in onset of skin lesion among SMS patients is of interest and the mechanism in this mouse model remains to be elucidated.

The appearance of skin lesion was erosive with scaly-red and white plaques located mostly on the back and tail and sometimes on the head, foot and ear (Fig. 1a). Generally, in psoriasis patients, skin lesion tends to develop at head, hip and the extensor side of joints such as wrists, elbows and knees where are susceptible to mechanical stress, which is known as Koebner phenomenon. The model here could also imply the role of mechanical stress to trigger the onset of cutaneous inflammation and in future studies, additional mechanical stress such as tape-stripping should be examined.

Histological analysis of the skin lesion of hR E373A mice revealed acanthosis, hyperkeratosis, parakeratosis and elongated rete ridges that are compatible with histological features of psoriasis (Fig. 5A). These features were consistent with the higher expression of keratinocytes hyperproliferation markers genes *K6, K16, Ki67* and the K5 abundance in suprabasal layers (Fig. 5C and Fig. 6). Cytokine profile of the skin revealed upregulation of *Tnfa, Il6* and IL-23/IL-17 axis cytokines that are primarily responsible cytokines for psoriasis. Infiltrating cells consist of neutrophils, dendritic cell and T cells, some of which also confers Th17 signature. *Mcp1* and *Vegf* genes were significantly upregulated in the skin lesion of hR E373A mice (Fig. 6), indicating excess dermal vascularity, which is one of the major characteristics of skin psoriasis (55). These pathological and cytokine profile findings in this mouse model are consistent with resemblance to human psoriasis.

In addition to monogenic disease cases, the role of RIG-I in the development of psoriasis in general was recently proposed by Huiyuan *et al* (56). They reported that stimulation of WT mice ears with a RIG-I ligand, 5'ppp-dsRNA, caused skin lesion resembling human psoriasis. It was

also shown that RIG-I is required for the development of psoriasis-like skin lesion in both IL-23 and IMQ stimulation(56). These stimulations should be tested in my model to boost the skin phenotypes and also to further support the idea of general involvement of RIG-I activation in the pathogenesis of psoriatic skin lesion.

IL-23 is produced from dendritic cells and can promote the differentiation of Th17 cells from naïve T cells (57). Repeated intradermal injection of IL-23 resulted in acanthosis and skin inflammation (58). Here, I found infiltration of $CD11c^+$ dendritic cells in the dermis and epidermis and high expression of IL-23/IL-17 axis cytokines in the psoriasis-like skin lesion. The mRNA expression levels of *Il6* and *Tgfb*, which promote Th17 differentiation through activating STAT3 to induce expression of RORγt (59-61), were greatly enhanced and $CD4^+$ cells co-stained with RORγt were detected in the affected skin (Fig. 8B), which suggests the involvement of Th17 cells in the skin lesion of hR E373A mice. Moreover, IL-17A deficiency totally canceled the of skin phenotype in hR E373A mice (Fig. 9A), indicating the essential role of IL-17A in the pathogenesis. Taken all together with previous reports which revealed the association of RIG-I to psoriasis, I propose that RIG-I could be involved in not only psoriatic cutaneous phenotypes in SMS but also psoriasis in general, both of which possibly share similar pathological mechanism.

Though skin lesion was still noticed in hR E373A *Rag2*$^{-/-}$ mice, the incidence was significantly lower and the lesion was less erosive and smaller in size. Histological analysis of the affected skin in hR E373A *Rag2*$^{-/-}$ mice showed milder psoriatic features compared to hR E373A *Rag2*$^{+/+}$, *i.e.*, the average epidermal thickness (acanthosis) decreased by around half, hyperkeratosis looked less severe and parakeratosis and rete-like elongations were absent (Fig. 11A and 12), which was compatible with the decreased expression of cutaneous inflammatory cytokines. Of note, IL-22, a cytokine which promotes keratinocytes proliferation and

differentiation (25), was preserved in hR E373A *Rag2*$^{-/-}$ mice compared to WT mice (Fig. 12B). This could explain the milder but remaining epidermal hyperplasia observed in hR E373A *Rag2*$^{-/-}$ mice. Additionally, this suggests the possible involvement of group 3 innate lymphoid cells (ILC3s) existing in hR E373A *Rag2*$^{-/-}$ mice as source of IL-22 in psoriasis-like skin lesion of the mice. Similarly, despite being significantly downregulated, *Il17a* was still detectable in the skin lesion of hR E373A *Rag2*$^{-/-}$ (Fig. 12B), adding further evidence of the importance of innate immune cells contribution in IL-17 production, including neutrophils, NK cells, mast cells and innate lymphoid cells (62-65).

To further address the role of IL-17 in the development of skin lesion, I treated mice with broad spectrum antibiotics (BSA) from the age of 3 weeks until they became 20 weeks old. Recent studies reported a link between commensal microbiota and many autoimmune diseases including Ankylosing spondylitis (66), inflammatory bowel disease, celiac disease, type-1 diabetes and rheumatoid arthritis (67). Additionally, gut microbiota have also been linked with psoriasis by modulating Th17 response (37). In hR E373A mice here, broad spectrum antibiotics treatment improved the incidence of skin lesion and histological severity (Fig. 13C and 14B). Though the IL-23/IL-17 axis cytokines were downregulated in the skin lesion of the transgenic mice treated with BSA, they were still significantly high compared to wt control (Fig. 14D). Despite this histological improvement, the clinical adaptation of BSA is controversial because antibiotics in neonatal life could increase murine susceptibility to experimental psoriasis (68).

Biological agents targeting IL-23/IL-17 axis has been approved for clinical use (69, 70). Tofacitinib, a JAK1 and JAK3 inhibitor, which blocks not only type I interferon but also various cytokine signaling, has been reported to improve psoriasis (71, 72). Here, the tofacitinib treatment from the age of 3 weeks prevented hR E373A mice from developing-like skin lesion and

suppressed systemic inflammation, as shown in the downregulation of the expression of T cell activation marker, CD69 (Fig. 15). More importantly, tofacitinib treatment after the onset of the skin lesion improved the skin phenotype (Fig. 16), indicating that JAK inhibitor treatment can be suggested as an effective treatment for cutaneous symptoms in SMS.

In summary, the data provide another evidence for the implication of RIG-I in the development of psoriasis. The data support prior work demonstrating a crucial role of IL-23/IL17 axis pathway in the development of skin psoriasis.

Chapter 5

REFERENCES

1. Takeuchi O, Akira S. Pattern recognition receptors and inflammation. Cell. 2010;140(6):805-20.
2. Yoo JS, Kato H, Fujita T. Sensing viral invasion by RIG-I like receptors. Curr Opin Microbiol. 2014;20:131-8.
3. Nejentsev S, Walker N, Riches D, Egholm M, Todd JA. Rare variants of IFIH1, a gene implicated in antiviral responses, protect against type 1 diabetes. Science. 2009;324(5925):387-9.
4. Varzari A, Bruch K, Deyneko IV, Chan A, Epplen JT, Hoffjan S. Analysis of polymorphisms in RIG-I-like receptor genes in German multiple sclerosis patients. J Neuroimmunol. 2014;277(1-2):140-4.
5. Zhu H, Lou F, Yin Q, Gao Y, Sun Y, Bai J, et al. RIG-I antiviral signaling drives interleukin-23 production and psoriasis-like skin disease. 2017;9(5):589-604.
6. Suarez-Calvet X, Gallardo E, Nogales-Gadea G, Querol L, Navas M, Diaz-Manera J, et al. Altered RIG-I/DDX58-mediated innate immunity in dermatomyositis. J Pathol. 2014;233(3):258-68.
7. Ferreira RC, Pan-Hammarstrom Q, Graham RR, Gateva V, Fontan G, Lee AT, et al. Association of IFIH1 and other autoimmunity risk alleles with selective IgA deficiency. Nat Genet. 2010;42(9):777-80.
8. Cunninghame Graham DS, Morris DL, Bhangale TR, Criswell LA, Syvanen AC, Ronnblom L, et al. Association of NCF2, IKZF1, IRF8, IFIH1, and TYK2 with systemic lupus erythematosus. PLoS Genet. 2011;7(10):e1002341.
9. Silva JA, Lima SC, Addobbati C, Moura R, Brandao LA, Pancoto JA, et al. Association of interferon-induced helicase C domain (IFIH1) gene polymorphisms with systemic lupus erythematosus and a relevant updated meta-analysis. Genet Mol Res. 2016;15(4).
10. Robinson T, Kariuki SN, Franek BS, Kumabe M, Kumar AA, Badaracco M, et al. Autoimmune disease risk variant of IFIH1 is associated with increased sensitivity to IFN-alpha and serologic autoimmunity in lupus patients. Journal of immunology. 2011;187(3):1298-303.
11. Funabiki M, Kato H, Miyachi Y, Toki H, Motegi H, Inoue M, et al. Autoimmune disorders associated with gain of function of the intracellular sensor MDA5. Immunity. 2014;40(2):199-212.
12. Soda N, Sakai N, Kato H, Takami M, Fujita T. Singleton-Merten Syndrome-like Skeletal Abnormalities in Mice with Constitutively Activated MDA5. Journal of immunology (Baltimore, Md : 1950). 2019;203(5):1356-68.
13. Oda H, Nakagawa K, Abe J, Awaya T, Funabiki M, Hijikata A, et al. Aicardi-Goutieres syndrome is caused by IFIH1 mutations. American journal of human genetics. 2014;95(1):121-5.
14. de Carvalho LM, Ngoumou G, Park JW, Ehmke N, Deigendesch N, Kitabayashi N, et al. Musculoskeletal Disease in MDA5-Related Type I Interferonopathy: A Mendelian Mimic of Jaccoud's Arthropathy. Arthritis & rheumatology (Hoboken, NJ). 2017;69(10):2081-91.
15. McLellan KE, Martin N, Davidson JE, Cordeiro N, Oates BD, Neven B, et al. JAK 1/2 Blockade in MDA5 Gain-of-Function. Journal of clinical immunology. 2018;38(8):844-6.
16. Enevold C, Kjaer L, Nielsen CH, Voss A, Jacobsen RS, Hermansen ML, et al. Genetic polymorphisms of dsRNA ligating pattern recognition receptors TLR3, MDA5, and RIG-I. Association with systemic lupus erythematosus and clinical phenotypes. Rheumatol Int. 2014;34(10):1401-8.
17. Tsoi LC, Spain SL, Knight J, Ellinghaus E, Stuart PE, Capon F, et al. Identification of 15 new psoriasis susceptibility loci highlights the role of innate immunity. Nat Genet. 2012;44(12):1341-8.
18. Ghadiam H, Mungee S. Singleton Merten Syndrome: A Rare Cause of Early Onset Aortic Stenosis. Case reports in cardiology. 2017;2017:8197954.
19. Feigenbaum A, Muller C, Yale C, Kleinheinz J, Jezewski P, Kehl HG, et al. Singleton-Merten syndrome: an autosomal dominant disorder with variable expression. Am J Med Genet A. 2013;161A(2):360-70.
20. Rutsch F, MacDougall M, Lu C, Buers I, Mamaeva O, Nitschke Y, et al. A specific IFIH1 gain-of-function mutation causes Singleton-Merten syndrome. American journal of human genetics. 2015;96(2):275-82.

21. Takeichi T, Katayama C, Tanaka T, Okuno Y, Murakami N, Kono M. A novel IFIH1 mutation in the pincer domain underlies the clinical features of both Aicardi-Goutieres and Singleton-Merten syndromes in a single patient. 2018;178(2):e111-e3.
22. Pettersson M, Bergendal B, Norderyd J, Nilsson D, Anderlid BM, Nordgren A, et al. Further evidence for specific IFIH1 mutation as a cause of Singleton-Merten syndrome with phenotypic heterogeneity. Am J Med Genet A. 2017;173(5):1396-9.
23. Jang MA, Kim EK, Now H, Nguyen NT, Kim WJ, Yoo JY, et al. Mutations in DDX58, which encodes RIG-I, cause atypical Singleton-Merten syndrome. American journal of human genetics. 2015;96(2):266-74.
24. Lassig C, Matheisl S, Sparrer KM, de Oliveira Mann CC, Moldt M, Patel JR, et al. ATP hydrolysis by the viral RNA sensor RIG-I prevents unintentional recognition of self-RNA. Elife. 2015;4.
25. Boniface K, Bernard FX, Garcia M, Gurney AL, Lecron JC, Morel F. IL-22 inhibits epidermal differentiation and induces proinflammatory gene expression and migration of human keratinocytes. Journal of immunology. 2005;174(6):3695-702.
26. Sakkas LI, Bogdanos DP. Are psoriasis and psoriatic arthritis the same disease? The IL-23/IL-17 axis data. Autoimmunity reviews. 2017;16(1):10-5.
27. Khairutdinov VR, Mikhailichenko AF, Belousova IE, Kuligina ES, Samtsov AV, Imyanitov EN. The role of intradermal proliferation of T-cells in the pathogenesis of psoriasis. Anais brasileiros de dermatologia. 2017;92(1):41-4.
28. Karczewski J, Dobrowolska A, Rychlewska-Hanczewska A, Adamski Z. New insights into the role of T cells in pathogenesis of psoriasis and psoriatic arthritis. Autoimmunity. 2016;49(7):435-50.
29. Di Meglio P, Villanova F, Navarini AA, Mylonas A, Tosi I, Nestle FO, et al. Targeting CD8(+) T cells prevents psoriasis development. The Journal of allergy and clinical immunology. 2016;138(1):274-6.e6.
30. Jetten AM, Cook DN. (Inverse) Agonists of Retinoic Acid-Related Orphan Receptor γ: Regulation of Immune Responses, Inflammation, and Autoimmune Disease. Annu Rev Pharmacol Toxicol. 2020;60:371-90.
31. Zhou L, Ivanov, II, Spolski R, Min R, Shenderov K, Egawa T, et al. IL-6 programs T(H)-17 cell differentiation by promoting sequential engagement of the IL-21 and IL-23 pathways. Nature immunology. 2007;8(9):967-74.
32. Russell SL, Gold MJ, Hartmann M, Willing BP, Thorson L, Wlodarska M, et al. Early life antibiotic-driven changes in microbiota enhance susceptibility to allergic asthma. EMBO reports. 2012;13(5):440-7.
33. Vaahtovuo J, Munukka E, Korkeamäki M, Luukkainen R, Toivanen P. Fecal microbiota in early rheumatoid arthritis. The Journal of rheumatology. 2008;35(8):1500-5.
34. Soyucen E, Gulcan A, Aktuglu-Zeybek AC, Onal H, Kiykim E, Aydin A. Differences in the gut microbiota of healthy children and those with type 1 diabetes. Pediatrics international : official journal of the Japan Pediatric Society. 2014;56(3):336-43.
35. Gao Z, Tseng CH, Strober BE, Pei Z, Blaser MJ. Substantial alterations of the cutaneous bacterial biota in psoriatic lesions. PloS one. 2008;3(7):e2719.
36. Zákostelská Z, Málková J, Klimešová K, Rossmann P, Hornová M, Novosádová I, et al. Intestinal Microbiota Promotes Psoriasis-Like Skin Inflammation by Enhancing Th17 Response. PloS one. 2016;11(7):e0159539.
37. Zakostelska Z, Malkova J, Klimesova K, Rossmann P, Hornova M, Novosadova I, et al. Intestinal Microbiota Promotes Psoriasis-Like Skin Inflammation by Enhancing Th17 Response. PloS one. 2016;11(7):e0159539.
38. Fleischmann R, Kremer J, Cush J, Schulze-Koops H, Connell CA, Bradley JD, et al. Placebo-Controlled Trial of Tofacitinib Monotherapy in Rheumatoid Arthritis. 2012;367(6):495-507.

39. Chang BY, Zhao F, He X, Ren H, Braselmann S, Taylor V, et al. JAK3 inhibition significantly attenuates psoriasiform skin inflammation in CD18 mutant PL/J mice. Journal of immunology (Baltimore, Md : 1950). 2009;183(3):2183-92.
40. D'Amico F, Parigi TL, Fiorino G, Peyrin-Biroulet L, Danese S. Tofacitinib in the treatment of ulcerative colitis: efficacy and safety from clinical trials to real-world experience. Therap Adv Gastroenterol. 2019;12:1756284819848631-.
41. Dhillon S. Tofacitinib: A Review in Rheumatoid Arthritis. Drugs. 2017;77(18):1987-2001.
42. Welsch K, Holstein J, Laurence A, Ghoreschi K. Targeting JAK/STAT signalling in inflammatory skin diseases with small molecule inhibitors. European journal of immunology. 2017;47(7):1096-107.
43. Naldi L, Mercuri SR. Epidemiology of comorbidities in psoriasis. Dermatologic therapy. 2010;23(2):114-8.
44. Alinaghi F, Calov M, Kristensen LE, Gladman DD, Coates LC, Jullien D, et al. Prevalence of psoriatic arthritis in patients with psoriasis: A systematic review and meta-analysis of observational and clinical studies. Journal of the American Academy of Dermatology. 2019;80(1):251-65.e19.
45. Springate DA, Parisi R, Kontopantelis E, Reeves D, Griffiths CE, Ashcroft DM. Incidence, prevalence and mortality of patients with psoriasis: a U.K. population-based cohort study. The British journal of dermatology. 2017;176(3):650-8.
46. Chandran V, Raychaudhuri SP. Geoepidemiology and environmental factors of psoriasis and psoriatic arthritis. Journal of autoimmunity. 2010;34(3):J314-21.
47. Menter A, Gottlieb A, Feldman SR, Van Voorhees AS, Leonardi CL, Gordon KB, et al. Guidelines of care for the management of psoriasis and psoriatic arthritis: Section 1. Overview of psoriasis and guidelines of care for the treatment of psoriasis with biologics. J Am Acad Dermatol. 2008;58(5):826-50.
48. Patrick MT, Stuart PE, Raja K, Gudjonsson JE, Tejasvi T, Yang J, et al. Genetic signature to provide robust risk assessment of psoriatic arthritis development in psoriasis patients. Nature communications. 2018;9(1):4178.
49. Strange A, Capon F, Spencer CC, Knight J, Weale ME, Allen MH, et al. A genome-wide association study identifies new psoriasis susceptibility loci and an interaction between HLA-C and ERAP1. Nature genetics. 2010;42(11):985-90.
50. Takeichi T, Katayama C, Tanaka T, Okuno Y, Murakami N, Kono M, et al. A novel IFIH1 mutation in the pincer domain underlies the clinical features of both Aicardi-Goutieres and Singleton-Merten syndromes in a single patient. The British journal of dermatology. 2018;178(2):e111-e3.
51. Rutsch F, MacDougall M, Lu C, Buers I, Mamaeva O, Nitschke Y, et al. A specific IFIH1 gain-of-function mutation causes Singleton-Merten syndrome. Am J Hum Genet. 2015;96(2):275-82.
52. Liu HM, Jiang F, Loo YM, Hsu S, Hsiang TY, Marcotrigiano J, et al. Regulation of Retinoic Acid Inducible Gene-I (RIG-I) Activation by the Histone Deacetylase 6. EBioMedicine. 2016;9:195-206.
53. Suh HS, Choi S, Khattar P, Choi N, Lee SC. Histone deacetylase inhibitors suppress the expression of inflammatory and innate immune response genes in human microglia and astrocytes. Journal of neuroimmune pharmacology : the official journal of the Society on NeuroImmune Pharmacology. 2010;5(4):521-32.
54. Ivashkiv LB, Donlin LT. Regulation of type I interferon responses. Nature reviews Immunology. 2014;14(1):36-49.
55. Marina ME, Roman, II, Constantin AM, Mihu CM, Tataru AD. VEGF involvement in psoriasis. Clujul medical (1957). 2015;88(3):247-52.
56. Zhu H, Lou F, Yin Q, Gao Y, Sun Y, Bai J, et al. RIG-I antiviral signaling drives interleukin-23 production and psoriasis-like skin disease. EMBO molecular medicine. 2017;9(5):589-604.

57. Langrish CL, Chen Y, Blumenschein WM, Mattson J, Basham B, Sedgwick JD, et al. IL-23 drives a pathogenic T cell population that induces autoimmune inflammation. The Journal of experimental medicine. 2005;201(2):233-40.
58. Chan JR, Blumenschein W, Murphy E, Diveu C, Wiekowski M, Abbondanzo S, et al. IL-23 stimulates epidermal hyperplasia via TNF and IL-20R2-dependent mechanisms with implications for psoriasis pathogenesis. The Journal of experimental medicine. 2006;203(12):2577-87.
59. Korn T, Bettelli E, Oukka M, Kuchroo VK. IL-17 and Th17 Cells. Annual review of immunology. 2009;27:485-517.
60. Ivanov, II, McKenzie BS, Zhou L, Tadokoro CE, Lepelley A, Lafaille JJ, et al. The orphan nuclear receptor RORgammat directs the differentiation program of proinflammatory IL-17+ T helper cells. Cell. 2006;126(6):1121-33.
61. Chen Z, O'Shea JJ. Th17 cells: a new fate for differentiating helper T cells. Immunologic research. 2008;41(2):87-102.
62. Lin AM, Rubin CJ, Khandpur R, Wang JY, Riblett M, Yalavarthi S, et al. Mast cells and neutrophils release IL-17 through extracellular trap formation in psoriasis. Journal of immunology (Baltimore, Md : 1950). 2011;187(1):490-500.
63. Blauvelt A, Chiricozzi AJCRiA, Immunology. The Immunologic Role of IL-17 in Psoriasis and Psoriatic Arthritis Pathogenesis. 2018;55(3):379-90.
64. Ueyama A, Imura C, Fusamae Y, Tsujii K, Furue Y, Aoki M, et al. Potential role of IL-17-producing CD4/CD8 double negative alphabeta T cells in psoriatic skin inflammation in a TPA-induced STAT3C transgenic mouse model. Journal of dermatological science. 2017;85(1):27-35.
65. Keijsers RR, Joosten I, van Erp PE, Koenen HJ, van de Kerkhof PC. Cellular sources of IL-17 in psoriasis: a paradigm shift? Exp Dermatol. 2014;23(11):799-803.
66. Babaie F, Hasankhani M, Mohammadi H, Safarzadeh E, Rezaiemanesh A, Salimi R, et al. The role of gut microbiota and IL-23/IL-17 pathway in ankylosing spondylitis immunopathogenesis: New insights and updates. Immunology letters. 2018;196:52-62.
67. Tlaskalova-Hogenova H, Stepankova R, Kozakova H, Hudcovic T, Vannucci L, Tuckova L, et al. The role of gut microbiota (commensal bacteria) and the mucosal barrier in the pathogenesis of inflammatory and autoimmune diseases and cancer: contribution of germ-free and gnotobiotic animal models of human diseases. Cellular & molecular immunology. 2011;8(2):110-20.
68. Zanvit P, Konkel JE, Jiao X, Kasagi S, Zhang D, Wu R, et al. Antibiotics in neonatal life increase murine susceptibility to experimental psoriasis. Nature communications. 2015;6:8424.
69. Boutet MA, Nerviani A, Gallo Afflitto G, Pitzalis C. Role of the IL-23/IL-17 Axis in Psoriasis and Psoriatic Arthritis: The Clinical Importance of Its Divergence in Skin and Joints. International journal of molecular sciences. 2018;19(2).
70. Chan TC, Hawkes JE, Krueger JG. Interleukin 23 in the skin: role in psoriasis pathogenesis and selective interleukin 23 blockade as treatment. Therapeutic advances in chronic disease. 2018;9(5):111-9.
71. Ma A-H-L, Masek-Hammerman A-K, Fish A-S, Napierata A-L, Nagiec A-E, Rahman A-S, et al. Attenuating Janus Kinases (JAK) by Tofacitinib Effectively Prevented Psoriasis Pathology in Various Mouse Skin Inflammation Models. Journal of Clinical & Cellular Immunology. 2013;4.
72. Papp KA, Menter A, Strober B, Langley RG, Buonanno M, Wolk R, et al. Efficacy and safety of tofacitinib, an oral Janus kinase inhibitor, in the treatment of psoriasis: a Phase 2b randomized placebo-controlled dose-ranging study. The British journal of dermatology. 2012;167(3):668-77.

Table 1: SYBR Green primer set sequences used in qRT-PCR analysis

Gene	Sequence (Forward)	Sequence (Reverse)
Gapdh	5′-CCCCAGCAAGGACACTGAGCAAG	GGGGTCTGGGATGGAAATTGTGAGG-3′
K6	5′-GTGGCCTCAGCTCTTCTACC	TCTGAGCACGGGATTCTGC -3′
K16	5′-AGAACCGCAGAGATGTGGAG	CTGCTGATCAAACCCTGGAT-3′
Mcp1	5′-AAAAACCTGGATCGGAACCAA	CGGGTCAACTTCACATTCAAAG-3′
Vegf	5′-CACGACAGAAGGAGAGCAGAAG	CTCAATCGGACGGCAGTAGC-3′
Cd45	5′-ATGGTCCTCTGAATAAAGCCCA	TCAGCACTATTGGTAGGCTCC-3′
Cd11c	5′-GCACCCAAAAGTTGCTG	AGCAGCCATGACCAGTTTAC-3′
Gr1	5′-TGCTCTTGACTTTGCTTCTGTGA	TGCCCCTTCTCTGATGGATT-3′
Il6	5′-CATGTTCTCTGGGAAATCGTGG	GTACTCCAGGTAGCTATGGTAC-3′
Tnfa	5′-GGCATGGATCTCAAAGACAACC	CAGGTATATGGGCTCATACCAG-3′
Il1b	5′-CATCCAGCTTCAAATCTCGCAG	CACACACCAGCAGGTTATCATC-3′
Il23	5′-AGCAACTTCACACCTCCCTAC	ACTGCTGACTAGAACTCAGGC-3′
Ifng	5′-CTGAGACAATGAACGCTACACA	TTTCTTCCACATCTATGCCACT-3′
Tgfb	5′-GGAGAGCCCTGGATACCAAC	CAACCCAGGTCCTTCCTAAA-3′
Il17	5′-TTTAACTCCCTTGGCGCAAAA	CTTTCCCTCCGCATTGACAC-3′
Il22	5′-ATCGTCAACCGCACCTTTAT	GACTCCTCGGAACAGTTTCTC-3′
16s	5′-AGAGTTTGATCCTGGCTCAG	CTGCTGCCTCCCGTAGGAGT-3′

Chapter 6

ACKNOWLEGMENTS

First, I would like to thank Prof. Takashi Fujita who kindly accepted me in his laboratory, and provided me with knowledge, guidance and support through my PhD studies. It has been an honour for me to work in his lab. I also thank Prof. Hiroki Kato for his dedicated support and guidance and whose insight and knowledge steered me through this research. I also thank Dr. Masahide Funabiki for his support and guidance during the running of this project. From the bottom of my heart, I would like to say big thank you for all my laboratory colleagues and research group members for their help throughout my study. Finally, I would like to thank my wife,Jumana Khalil, and my family for their patience and encouragement.

This study was supported by independent grants from the Japan Science and Technology Agency, from the Ministry of Education, Culture, Sports, Science and Technology of Japan (innovative areas, infection competency, 24115004), Japan Agency for Medical Research and Development under grants JP17ek0109100h0003 and JP18ek0109387h0001, The Kato Memorial Trust for Nambyo Research, and the Japan Society for the Promotion of Science Core to Core Program. It was also funded by the Deutsche Forschungsgemeinschaft (German Research Foundation) under Germany's Excellence Strategy – EXC2151 – 390873048 and TRR237, and also by the Deutsche Forschungsgemeinschaft (German Research Foundation) Grant No. 369799452 – Project number 404459591.

This thesis is based on material contained in the following scholarly paper: Ahmed Abu Tayeh, Masahide Funabiki, Shota Shimizu, Saya Satoh, Lee Sumin, Yoichiro Iwakura, Hiroki Kato and Takashi Fujita

Psoriasis-like skin disorder in transgenic mice expressing a RIG-I Singleton-Merten syndrome variant

International Immunology, October 2020, doi.org/10.1093/intimm/dxaa071